TIR 2114-MED-5004

A SYSTEMS ANALYSIS OF THE ERYTHROPOIETIC RESPONSES TO WEIGHTLESSNESS

VOL. II DESCRIPTION OF THE MODEL OF ERYTHROPOIESIS REGULATION

PART A. MODEL FOR REGULATION OF ERYTHROPOIESIS

PART B. DETAILED DESCRIPTION OF THE MODEL FOR REGULATION OF ERYTHROPOIESIS

Joel I. Leonard, Ph.D.

Management and Technical Services Company

Houston, Texas

1985

PART A.

MODEL FOR REGULATION OF ERYTHROPOIESIS

Model for Regulation of Erythropoiesis

A mathematical model of the erythropoiesis regulating system was developed for use as a tool to investigate the relative influence of the controlling factors of erythropoiesis on total red blood cell (RBC) mass. The loss of red cell mass has been a consistent finding during space flight and certain ground-based analogs of weightlessness such as bed rest. Computer simulation of this phenomenon required a model that could account for oxygen transport, red cell production, and red cell destruction.

The control of erythropoiesis is amenable to a modeling approach, as demonstrated by a variety of investigators. These models have ranged from conceptual, qualitative feedback schemes (refs. III-51 and III-52) to more detailed mathematical descriptions (ref. III-53), some of which have led to computer simulation models (refs. III-8 and III-54). Quantitative models have been developed for different aspects of erythropoiesis regulation, including ferrokinetic models (refs. III-55 and III-56) and those describing the control of stem cell production (refs. III-57 to III-59).

A limited number of models are available that integrate the entire feedback circuit in sufficient detail to enable quantitative simulation of diverse hematological stresses directly affecting oxygen transport, tissue oxygenation, erythropoietin release, and red cell production. Hodgson (ref. III-53) has proposed such a model but apparently has neither implemented it for computer use nor performed the studies necessary for validation. An algorithm capable of predicting red cell mass changes by feedback processes was coupled to a much larger model of circulatory and fluid control (ref. III-8), but it provided only a gross representation of the renal/bone-marrow axis and failed to recognize renal oxygenation as a major control element. The most complete simulation model previously developed is that of Mylrea and Abbrecht (ref. III-54); this model was validated for a single stress (altitude hypoxia in mice).

A review of the factors that control erythropoiesis and of existing models led to the formulation of a conceptual model and eventually the design and development of a computer model (ref. III-60). The initial structure was derived from the best features of the mathematical models of Guyton et al. (ref. III-8), Hodgson (ref. III-53), and Mylrea and Abbrecht (ref. III-54). The model has a wide range of applicability; the most important application is its simulation of space-flight events.

Model description—Those elements in the feedback regulation loop that have been incorporated into the model are shown schematically in figure III-27. The formulation is based on the accepted concept that erythrocyte production is governed by the balance between oxygen supply and demand in the body and, in particular, at a renal sensing site. The mechanisms and pathways of the control circuit include oxygenation of hemoglobin and oxygenation of tissues by blood transport and diffusional processes. An erythrocyte-stimulating hormone, erythropoietin, is produced and released at a renal site in amounts that vary inversely with the levels of tissue oxygen tension (pO_2). Plasma levels of erythropoietin control the production of erythrocytes in the bone marrow. The amount of circulating red cell mass is based on the addition of new cells to existing cells with allowance for the destruction of older cells. Blood hematocrit, an index of red cell concentration in whole blood, is determined by dividing the circulating red cell mass by the plasma volume. Other features of the model include an oxygen-hemoglobin affinity, which can be varied, and time delays which represent time for erythropoietin distribution in plasma and time for maturation of erythrocytes in the bone marrow.

*This section was originally written as part of a more comprehensive chapter on physiological models which is as yet unpublished. Figures, tables, equations, numbers, and references have been left intact from the original.

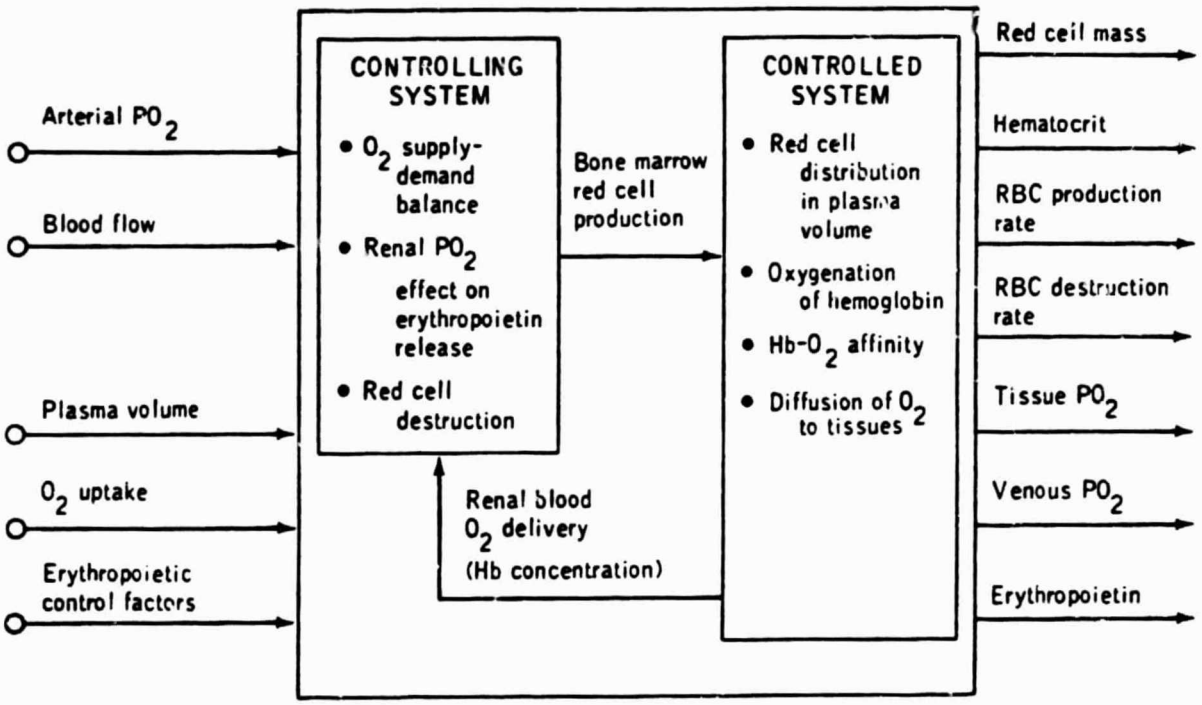

FIGURE III-27.—Schematic of the erythropoietic control system model.

In terms of control system theory, the controlled system includes the elements of redistribution of new cells, lung oxygenation, blood transport, and tissue oxygen extraction, whereas the controller system consists of erythropoietin release, marrow red cell production, and splenic destruction. The hematocrit (or hemoglobin level) may be considered to be the primary feedback quantity, and the level of tissue oxygenation can be taken as the directly controlled variable. Figure III-27 indicates the input parameters which have been found most useful in these studies, as well as the predicted output responses which the model is capable of generating. Appendix B and Section V contain a more complete description of the model system.

Sensitivity analysis—The effect of variation of the model parameters on the overall behavior of the system can be studied by sensitivity analysis techniques. (See app. A.) Sensitivity analysis is a systematic method of evaluating the relative importance of different parameters. Steady-state sensitivity coefficients were estimated by varying each of the most important parameters, one at a time, by small increments around the normal control state. Table III-6 contains the percent change in one dependent variable (red cell production rate) caused by a 1-percent decrease in the model parameters (shown in the left column) and determined after a new steady-state condition was reached. Positive values of these coefficients indicate a response to a hypoxic condition, and negative values indicate response to tissue hyperoxia. In each case, the response is in a direction that agrees with the concepts of erythropoiesis regulation (ref. III-61). The unusually high influence of oxygen uptake on red blood cell production indicated may not be representative of the real intact system. Compensatory action by cardiorespiratory factors usually intervene to normalize oxygen transport and thereby limit the correction required by the erythropoietic system (app. B). However, this analysis does support the assertion that *P*50 shifts can dramatically augment tissue oxygenation (refs. III-62 and III-63).

The results from a dynamic sensitivity analysis are illustrated in figure III-28. In this case, the six most important parameters were changed by 10 percent in a direction that would initiate a hypoxic response. The dynamic behavior of four important dependent system variables during this constant load disturbance is shown over a period of 30 days. It is apparent that the general ranking of parameter

TABLE III-6.—Steady-State Sensitivity Coefficients[a]

Parameter	*Change in red cell production, percent*
Oxygen demand, V_m	−4.55
O_2-Hb affinity, *P*50	3.90
Capillary diffusivity, K_d	3.25
Blood flow, Q	1.45
Mean corpuscular hemoglobin concentration, *MCHC*	1.45
Hemoglobin O_2 carrying capacity, *CHbO*	1.45
Arterial O_2 tension, P_aO	1.10
Plasma volume, *PV*	−.90
Red cell half-life, *TRHL*	.85
Controller gain, *G*	−.03

[a]Values shown are percent change in red cell production at steady state due to a 1-percent decrease in parameter value

importance found in the steady state is maintained for the dynamic state as well. If, however, a new equilibrium state was simulated for a specific hypoxia condition and sensitivity coefficients were obtained by small perturbations from that state, both the magnitude and the ranking of the coefficients might be altered. Such behavior would not be unexpected for a nonlinear control system.

Figure III-28 also illustrates the wide difference in dynamic properties of the various elements in the model. This model may be viewed as consisting of four sequential processes, each with a characteristic time constant that is correspondingly longer with respect to alterations in tissue oxygenation (seconds to minutes), erythropoietin release (hours), red cell production (days), and red cell mass (days to months). An interesting prediction of these simulations is that the dynamic characteristics of the hypoxia response are similar for a variety of constant load disturbances, whether it be an increase in plasma volume or a decrease in renal flow rate. Unfortunately, the experiments required to confirm this conclusion are difficult to perform. These simulation results should, therefore, be considered as model-to-model comparisons which demonstrate that the model responds appropriately in a gross sense to both equilibrium and dynamic states.

Model validation—Model-to-data comparison is a more challenging validation process which must be used to establish ultimate credibility of any

model system. The erythropoiesis control model has been validated for long-term altitude hypoxia.

Buderer and Pace (ref. III-64) studied the dynamic changes in red cell mass, hematocrit, and plasma volume in sea-level pigtailed monkeys during 6 months at 3800 meters altitude followed by descent to sea level for 3 months. Comparable data for human subjects were not available. However, the human model would not be expected to be fundamentally different from that for a monkey at sea level, especially if responses are expressed as normalized values. The major driving function for the model was an arterial blood oxygen tension of 6.7 and 12.7 kN/m^2 (50 and 95 mmHg) for the altitude and sea-level phases, respectively. The model's response was adjusted using the bone marrow controller gain until a visual "best fit" was obtained. This is an example of parameter estimation. (See app. E.) The comparison of model output and data are illustrated in figure III-29. In combination with the arterial blood oxygen tension, the experimentally determined change in plasma volume (bottom curve) was used as a driver for the simulation, but the effect on the overall response system for this secondary load input was relatively small.

In addition to predicting the measured dynamic changes of red cell mass and hematocrit, the model is capable of predicting other system variables that were not measured, such as plasma erythropoietin and red cell production-destruction rates. The simulation shows the general sequence of events, generally assumed to characterize the hypoxic response, including tissue hypoxia (not shown), elevated erythropoietin, and augmented red cell production levels, which increase the mass of circulating blood cells (refs. III-65 to III-67). Figure III-29 also shows the opposite scenario for the descent phase. The difference between production and destruction rates provides a visual indication of the dynamic behavior of deviation from steady state. The slow approach to equilibrium at altitude is also evident from the asymptotic nature of the measured quantities. Upon return to sea level, the increased hematocrit serves as a prolonged stimulus for tissue hyperoxia to the extent that red cell production may be totally inhibited for several weeks.

The erythropoietin response in humans and mice is known to return toward control more rapidly than indicated in figure III-29 (refs. III-65 and III-68). Adaptive mechanisms of the circulatory, ventilatory, and biochemical systems respond to hypoxia and thereby improve oxygen transport faster than does the more sluggish erythropoietic system (ref. III-69). Several simulations were performed to test the hypothesis that some of these pathways contribute to the observed erythropoietin response. Figure III-30 illustrates the relative influence of three adaptive mechanisms (an increase in pO_2 due to greater ventilation efficiency, a decreased plasma volume, and a diminished oxyhemoglobin affinity) as predicted by the model. These simulations, although not strictly a validation study, not only illustrate a more realistic response but also indicate the manner in which simulation techniques can be used to test hypotheses regarding physiological mechanisms.

Mouse model—Experiments with animals are routinely conducted in support of space-flight biomedical investigations. In particular, mice have been examined for their potential use as experimental models for the study of the early erythropoietic disturbances found in astronauts (ref. III-70). The desirability of using a species-specific model of erythropoiesis for predicting experimental results with animal subjects prompted the formulation of a "mouse model." This model was based on the human model but incorporated parameter values that describe the unique characteristics of the oxygen transport and erythropoietic system for the mouse. Thus, red cell lifespan, arterial oxygen tension, oxygen-hemoglobin affinity, and many other parameters were found to differ significantly from the human (ref. III-71 and app. B).

The mouse model was validated in a preliminary study by examining its responses to hypoxia (ref. III-70) and to erythropoietin infusions (ref. III-72). An example of the dynamic behavior of the mouse model is provided in figure III-31. In this simulation, a pulse decrease in arterial oxygen tension results in a corresponding disturbance in tissue oxygen levels, followed by a short burst of erythropoietin and a resulting wave of erythropoiesis, the effects of which may last 2 weeks or longer. The transient nature of red cell production shown here has been previously observed after injecting erythropoietin into mice (ref. III-73). A similar simulation performed with the human model results in more prolonged effects, as indicated in figure III-31. These differences result primarily from the shorter erythropoietin disappearance rates, red cell lifespan, and erythropoietin half-life in the mouse when compared to the

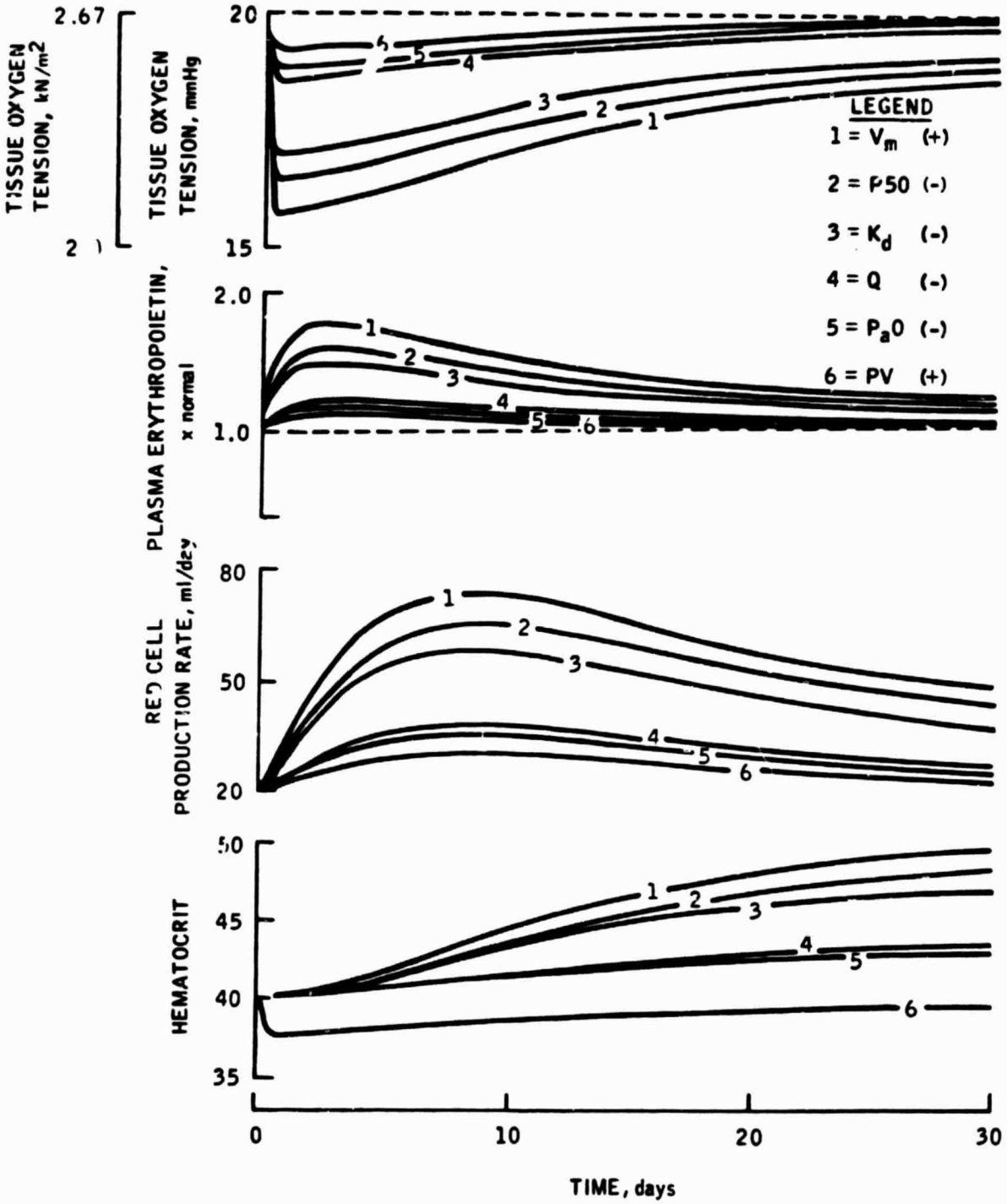

FIGURE III-28.—Hypoxic response of erythropoietic model to a 10-percent constant load disturbance (i.e., step change) of various parameters. Algebraic sign in legend refers to direction of change in each parameter. These simulations are useful for demonstrating dynamic behavior of model and relative sensitivities of important parameters.

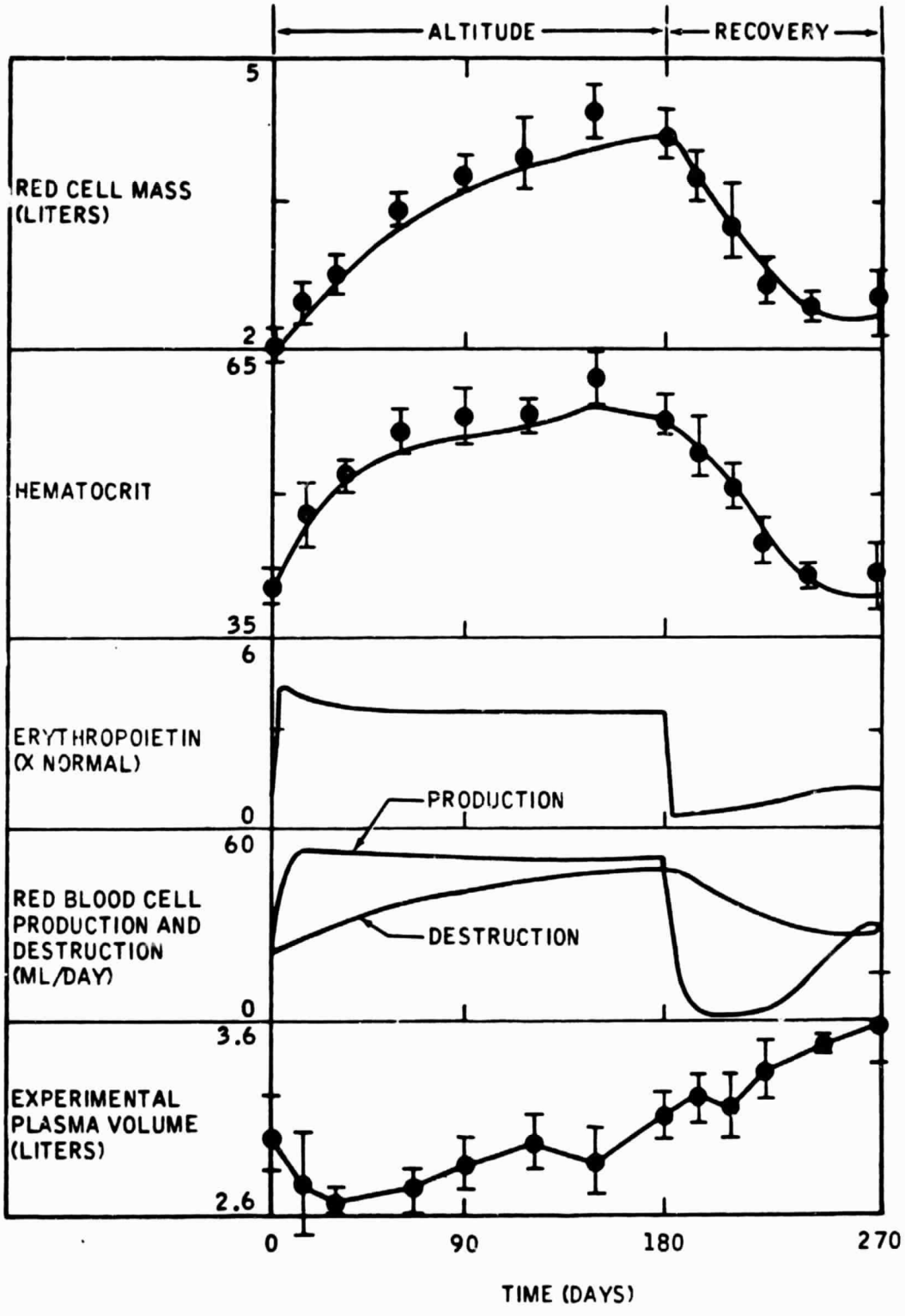

FIGURE III-29.—Simulation of altitude hypoxia and descent to sea level (solid lines). Experimental data from pigtailed monkeys (filled circles plus or minus standard error) were taken from reference III-64. Hypoxia was simulated by reducing arterial oxygen tension from 12.7 kN/m² (95 mmHg) (sea-level value) to 6.7 kN/m² (50 mmHg). At 180 days, arterial oxygen tension is returned to 12.7 kN/m² (95 mmHg). Experimental plasma volumes (bottom curve) were also used to drive model.

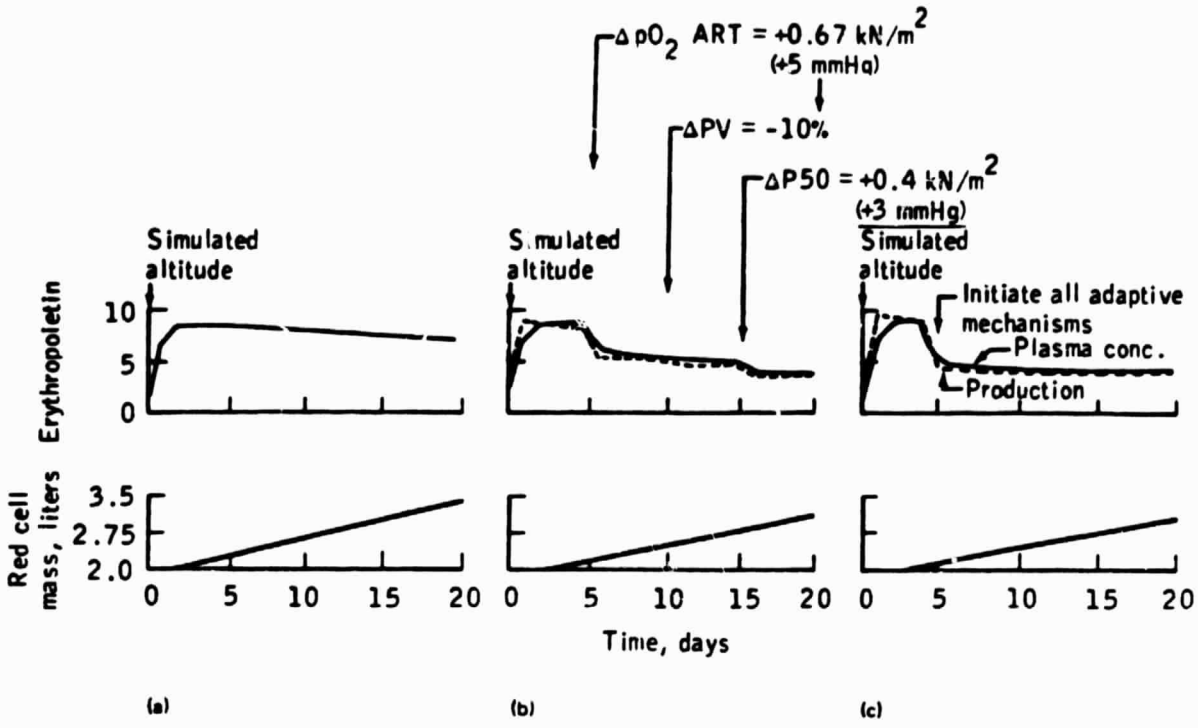

FIGURE III-30.—Simulation of altitude hypoxia showing effect of three adaptive mechanisms. (See text.) Models can be useful in studying several simultaneous stresses either in combination or acting alone. Simulated altitude = 4000 meters, pO_2 ART = arterial oxygen tension, PV = plasma volume, P50 = parameter describing oxygen-hemoglobin affinity. (a) No adaptive mechanisms. (b) Stepwise addition of three adaptive mechanisms. (c) Combined effect of three mechanisms.

human. Simulations such as this suggest that some information regarding erythropoiesis may be obtained in a shorter time interval using the mouse as an experimental model of the human.

Other simulations—Although the major purpose of the erythropoietic control model was to investigate mechanisms related to the loss of red cells during space flight, other applications have been investigated to validate the model, to test hypotheses, and to introduce refinements. Table III-7 is a summary of the major simulations accomplished with the human and mouse models. Human bed-rest and mouse dehydration studies have been found to be useful experimental analogs of space-flight effects. A more recent area of model development is in the simulation of hematological disease states which have known physiological etiologies (such as anemias, polycythemias, and abnormalities in hemoglobin functions). Toward this end, a steady-state model based on the dynamic model described previously has been formulated. A program is now in progress to develop a teaching model of pathophysiology based on the human red cell model.

Limitations—The erythropoiesis control system model is the least complex of all the models described in this section. Various features have been added during its development to increase its simulated realism. These have included elements representing erythropoietin release, cell maturation time delays, and a variable oxygen-hemoglobin affinity. Other limitations have been identified which either are acceptable within the scope of this program or form the basis for suggested improvements. These limitations are summarized here.

1. Red cell production is modulated by factors other than those considered in the model. These include iron levels, hormones other than erythropoietin, and neural stimulation, as well as inhibitors and activators of erythropoietin. Although it may be desirable to include these effects in future model applications, quantitative information regarding them is presently lacking or the need for their inclusion is not yet warranted

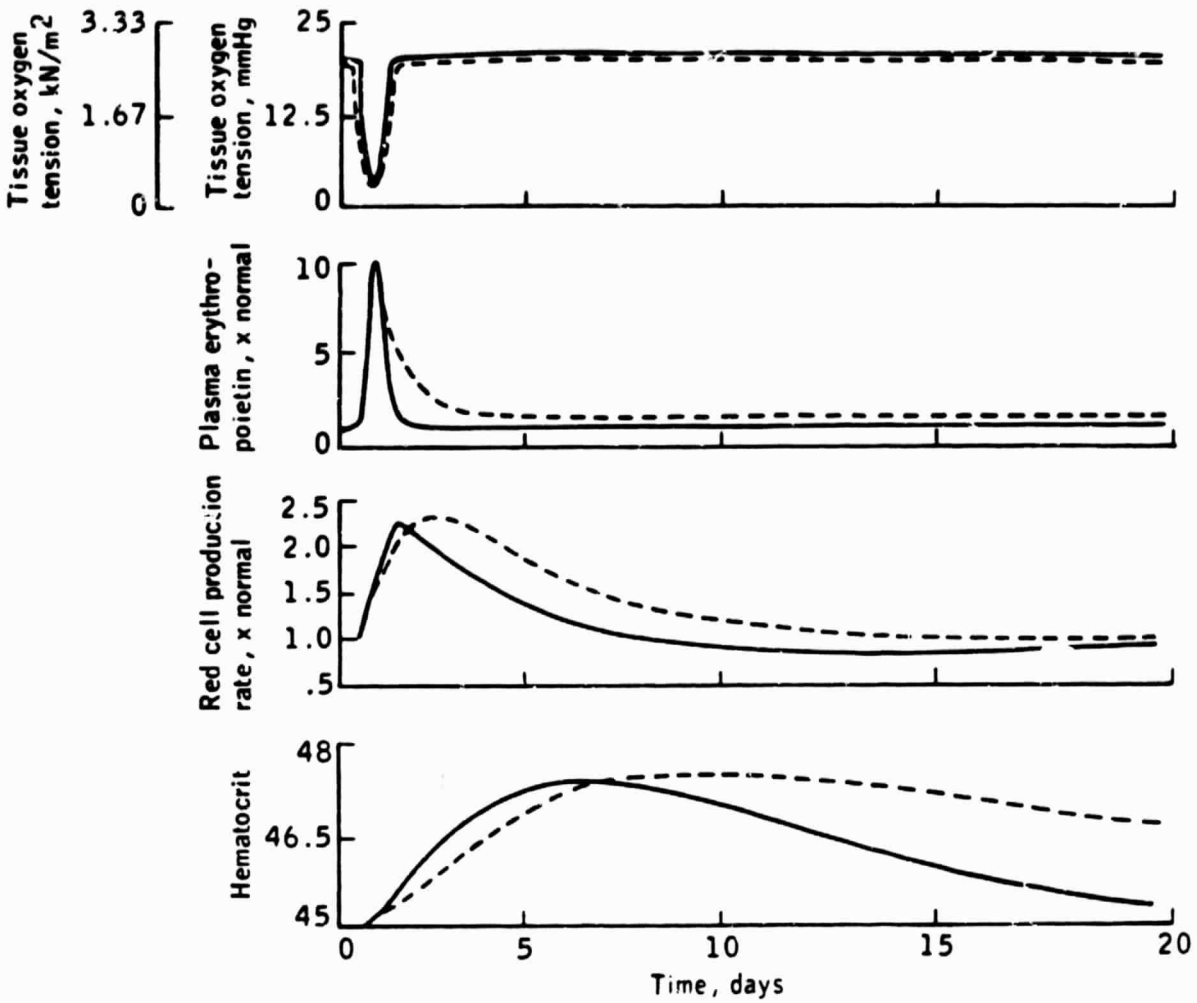

FIGURE III-31.—Simulation response to a pulse decrease in arterial oxygen tension for the mouse model (solid line) and the human model (dashed line).

2. The model has a limited representation of bone marrow red cell production. For example, it does not include the full maturation cycle from multipotential cells to denucleated red cells. Furthermore, it has no means of predicting reticulocyte index.

3. The model does not include extrarenal erythropoietin production or extramedullary erythropoiesis. These factors are of much greater importance in the mouse than in the human. However, sufficient quantitative information is lacking for inclusion in a mathematical model.

4. Blood viscosity and blood volume changes are known to influence blood flow and, thereby, tissue oxygenation. These effects are not explicitly represented in the model (refs. III-81 and III-82).

5. Overall oxygen transport is under the control of homeostatic mechanisms in addition to the erythropoiesis system. Thus, some of the fixed parameters of the model such as blood flow, capillary diffusivity, arterial oxygen tension, plasma volume, and oxygen-hemoglobin affinity can be considered variable elements of circulatory, ventilatory, biochemical, and fluid regulatory feedback mechanisms that are beyond the scope of the present model's design objectives.

Larger models that incorporate many of these features are available, and these have been shown

TABLE III-7.—Computer Simulation Studies Performed With Erythropoiesis Model

Study	Duration, days	Source
Human model		
Altitude hypoxia and descent	270	Ref. III-64
Altitude hypoxia	6	Ref. III-67
Red cell infusion	120	Ref. III-74
Bed rest	35	Refs. III-75, III-76
	14, 28	Ref. III-77
Skylab	59, 84	Ref. III-78
Clinical conditions	—	—
Anemia (primary, secondary, hemolytic)		
Polycythemia (primary, secondary, hypoxic)		
Abnormality (hemoglobin)		
Mouse model		
Multiple sequential erythropoietin infusion	7	Ref. III-73
Altitude hypoxia	28	Ref. III-68
Dehydration and recovery	7	Ref. III-79
Red cell infusion	3	Ref. III-80

REFERENCES

III-51. Fisher, J. W.; Busuttil, R.; et al.: The Kidney and Erythropoietin Production: A Review. Erythropoiesis—Proceedings of the Fourth International Conference on Erythropoiesis. K. Nakao, J. W. Fisher, and F. Takaku, eds., University Park Press, 1975, pp. 315-336.

III-52. Erslev, A. J.: Erythropoietin in Clinical Medicine. Erythropoiesis—Proceedings of the Fourth International Conference on Erythropoiesis. K. Nakao, J. W. Fisher, and F. Takaku, eds., University Park Press, 1975, pp. 425-433.

III-53. Hodgson, G.: Application of Control Theory to the Study of Erythropoiesis. Regulation of Hematopoiesis, Vol. I, ch. 15, A. S. Gordon, ed., Appleton-Century-Crofts (New York), 1970.

III-54. Mylrea, Kenneth C.; and Abbrecht, Peter H.: Mathematical Analysis and Digital Simulation of the Control of Erythropoiesis. J. Theor. Biol., vol. 33, no. 2, Nov. 1971, pp. 279-297.

III-55. Cavill, I.; and Ricketts, C.: The Kinetics of Iron Metabolism. Iron in Biochemistry and Medicine, A. Jacobs and M. Worwood, eds., Academic Press (London), 1974, pp. 613-647.

III-56. Berzuini, C.; Franzone, P. Colli; Stefanelli, M.; and Viganotti, C.: Iron Kinetics: Modelling and Parameter Estimation in Normal and Anemic States. Comp. & Biomed. Res., vol. 11, no. 3, 1978, pp. 209-228.

III-57. Mackey, M. C.: Unified Hypothesis for the Origin of Aplastic Anemia and Periodic Hematopoiesis. Blood, vol. 51, 1978, pp. 941-956.

III-58. Lajtha, L. G.; Oliver, R.; and Gurney, C. W.: Kinetic Model of a Bone-Marrow Stem-Cell Population. British J. Hematol., vol. 8, 1962, pp. 442-460.

III-59. Kretchmar, A. L.: Erythropoietin: Hypothesis of Action Tested by Analog Computer. Science, vol. 152, 1966, pp. 367-370.

III-60. Leonard, J. I.: Study Report—The Application of Systems Analysis and Mathematical Models to the Study of Erythropoiesis During Space Flight. Rep. TIR 741-MED-4012, General Electric Co. (Houston, Tex.), 1974.

III-61. Krantz, S. B.; and Jacobson, L. O.: Erythropoietin and the Regulation of Erythropoiesis. University of Chicago Press, 1970.

III-62. Brewer, G. J.: 2,3-DPG and Erythrocyte Oxygen Affinity. Ann. Rev. Med., vol. 25, 1975, pp. 29-38.

III-63. Metcalfe, James; and Dhindsa, Dharam S.: The Physiological Effects of Displacements of the Oxygen Dissociation Curve. Oxygen Affinity of Hemoglobin and Red Cell Acid Base Status, P. Astrup and M. Rorth, eds., Academic Press (New York), 1972, pp. 613-628.

III-64. Buderer, Melvin C.; and Pace, Nello: Hemopoiesis in the Pig-Tailed Monkey Macaca Nemestrina During Chronic Altitude Exposure. American J. Physiol., vol. 223, no. 2, 1972, pp. 346-352.

III-65. Abbrecht, Peter H.; and Littell, Judith K.: Plasma Erythropoietin in Men and Mice During Acclimatization to Different Altitudes. J. Appl. Physiol., vol. 32, no. 1, 1972, pp. 54-58.

III-66. Huff, R. L.; Lawrence, J. H.; et al.: Effects of Changes in Altitude on Hematopoietic Activity. Medicine (Baltimore), vol. 30, no. 3, Sept. 1951, pp. 197-217.

III-67. Faura, J.; Ramos, J.; et al.: Effect of Altitude on Erythropoiesis. Blood, vol. 33, May 1969, pp. 668-676.

III-68. Dunn, C. D. R.; Jarvis, J. H.; and Napier, J. A. F.: Changes in Erythropoiesis and Renal Ultrastructure During Exposure of Mice to Hypoxia. Exp. Hematol., vol. 4, no. 6, Nov. 1976, pp. 365-381.

III-69. Finch, Clement A.; and Lenfant, Claude: Oxygen Transport in Man. New England J. Med., vol. 286, no. 8, 1972, pp. 407-415.

III-70. Dunn, C. D. R.: Effect of Dehydration on Erythropoiesis in Mice: Relevance to the "Anemia" of Space Flight. Aviat. Space & Environ. Med., vol. 49, 1978, pp. 990-993.

III-71. Leonard, J. I. System Parameters for Erythropoiesis Control Model: Comparison of Normal Values in Human and Mouse Model. (General Electric Co., Houston, Tex.; TIR 741-LSP-8024.) NASA CR-160401, 1978.

III-72. Leonard, J. I.: Study Report—Improvements and Validation of the Erythropoiesis Control Model for the Simulation of Bed Rest. (General Electric Co., Houston, Tex.; TIR 741-LSP-7012.) NASA CR-160187, 1977.

III-73. Gurney, C. W.; Wackman, N.; and Filmanowicz, E.: Studies on Erythropoiesis. XVII. Some Quantitative Aspects of the Erythropoietic Response to Erythropoietin. Blood, vol. 17, May 1961, pp. 531-546.

III-74. Birkhill, F. R.; Maloney, M. A.; and Levenson, S. M.: Effect of Transfusion Polycythemia Upon Bone Marrow Activity and Erythrocyte Survival in Man. Blood, vol. 6, no. 11, Nov. 1951, pp. 1021-1033.

III-75. Morse, B. S.: Erythrokinetic Changes in Man Associated With Bed Rest. Lectures in Aerospace Medicine, 6th Series, School of Aerospace Medicine (Brooks Air Force Base, Tex.), 1967, pp. 240-254.

III-76. Lancaster, Malcolm C.: Hematologic Aspects of Bed Rest. Hypogravic and Hypodynamic Environments, Raymond H. Murray and Michael McCally, eds., Sec. IV, Metabolic Effects of Bed Rest, ch. 23. NASA SP-259, 1971, pp. 299-307.

III-77. Johnson, Philip C.; and Mitchell, Cheryl, compilers: Report of 28-Day Bedrest Simulation of Skylab, Vols. I and II, The Methodist Hospital (Houston, Tex.). NASA CR-151354, 1977.

III-78. Kimzey, S. L.: The Effects of Extended Spaceflight on Hematologic and Immunologic Systems. J. American Med. Women's Assoc., vol. 30, no. 5, May 1975, pp. 218-232.

III-79. Dunn, C. D. R.; and Lange, R. D.: Erythropoietic Effects of Space Flight. Acta Astronaut., vol. 6, May-June 1979, pp. 725-732.

III-80. Dunn, C. D. R.; and Lange, R. D.: Erythropoietic Effects of Space Flight Studied in a Potential Animal Model. Proceedings 50th Annual Aerospace Medical Association Meeting, 1979, pp. 14-15.

III-81. Castle, W. B.; and Jandle, T. H.: Blood Viscosity and Blood Volume: Opposing Influences Upon Oxygen Transport in Polycythemia. Seminars in Hematology, vol. 3, 1966, pp. 193-198.

III-82. Murphy, G. P.; Johnston, G. S.; and Scott, W. W.: The Effect of Arterial Hematocrit Alteration on Renal Blood Flow and Resistance in Normotensive States. J. Urol., vol. 95, Apr. 1966, pp. 453-464.

Also see: Leonard, J.I.; Kimzey, S.L., and Dunn, C.D.R.: Dynamic Regulation of Erythropoiesis; A Computer Model of General Applicability. Expt. Hematol., Vol. 9, 1981, pp. 355-378. (Primary source - Leonard, J.I. TIR 741-LSP-9005, General Electric Co., NASA CR-160203, 1979)

PART B.

DETAILED DESCRIPTION OF THE MODEL FOR REGULATION OF ERYTHROPOIESIS

* Detailed Description of the Model for Regulation of Erythropoiesis

The model developed for the space-flight hematological program was designed to examine the relative influence of the controlling factors of erythropoiesis on total red blood cell (RBC) mass. The formulation was based on the generally accepted concept that the overall balance between oxygen supply and demand regulates the release of a hormone, erythropoietin, from renal tissues sensitive to oxygen tension levels and that this substance in turn controls bone marrow red cell production (refs. B-1 to B-3).

The amount of oxygen delivered to the tissue is accounted for in the model by the combined influence of several factors: hemoglobin concentration, lung oxygenation of hemoglobin, blood flow, and oxygen-hemoglobin affinity (ref. B-4). From this amount of oxygen, a certain fraction is extracted by the tissue, depending on the oxygen demand parameter. Oxygen enters the cellular spaces by diffusion along an oxygen tension gradient between the venous capillaries and the cell (ref. B-5). Decreasing the oxygen supply in relation to the demand reduces tissue oxygen tension which is, in effect, monitored by a local oxygen detector (ref. B-6) and results in increased rates of erythropoietin release (ref. B-7). Erythropoietin is released into the general circulation, and its final plasma concentration is determined by its rate of release, its volume of distribution, and the rate at which it is metabolized (ref. B-8), the latter being represented in the model by the hormone plasma half-life. The target organ for erythropoietin is the bone marrow. The production rate and release of red cells in the model are determined by the plasma erythropoietin concentration (ref. B-9). A time delay exists between marrow stimulation and red cell release (ref. B-10). Destruction of cells is represented in the model by a lifespan parameter. Hemoglobin concentration in blood is based on the addition of new cells to existing cells and plasma.

It is known that red cell production is modulated by factors other than those considered in the model. These include iron levels (ref. B-11), hormones other than erythropoietin (ref. B-12), neural stimulation (ref. B-13), as well as inhibitors and activators of erythropoietin (ref. B-14). Although it may be desirable to include these effects in future model applications, quantitative information regarding them is presently lacking or the need for their inclusion is not yet warranted.

Overall oxygen transport is under the control of homeostatic mechanisms in addition to the erythropoiesis system. Thus, some of the fixed parameters of the model such as blood flow, capillary diffusivity, arterial oxygen tension, plasma volume, and oxygen-hemoglobin affinity can be considered variable elements of circulatory, ventilatory, biochemical, and fluid regulatory feedback mechanisms that are beyond the scope of the current model's design objectives. Larger models that incorporate many of these features are available and these have been shown to be compatible with an erythropoiesis subsystem model (ref. B-15). Although these mechanisms are not included explicitly in the present erythropoiesis model, their influence can be tested, in most cases, by manual alteration of existing model parameters.

MATHEMATICAL DESCRIPTION OF MODEL

Oxygenation of Blood

The oxygen concentration of arterial blood (neglecting oxygen dissolved in plasma) after passage through the lungs can be expressed as the product of the carrying capacity of a gram of hemoglobin (*CHbO*; i.e., 4 moles O_2 per mole *Hb*), times the hemoglobin concentration (*Hb*), times the fractional degree of oxygen-hemoglobin saturation (S_aO). It is convenient to use hematocrit rather than hemoglobin concentration as an index of red cell concentration in blood. These quantities are related by the mean corpuscular hemoglobin concentration, such that $MCHC = Hb/Hct$. Therefore, for arterial blood[1]

$$C_aO = S_aO \times Hb \times CHbO$$

$$= S_aO \times Hct \times MCHC \times CHbO \quad \text{(B1)}$$

[1]See table B-I for symbol definitions, units, and normal values.

*This section was originally written as part of a more comprehensive chapter on physiological models which is as yet unpublished. Figures, tables, equations, numbers, and references have been left intact from the original.

At full hemoglobin saturation, $S_aO = 1.0$ and equation (B1) then represents the maximum oxygen-carrying capacity of blood at a given hematocrit. In most instances, the parameters *MCHC* and *CHbO* will be invariant, so that the arterial oxygen concentration is influenced only by the hematocrit and hemoglobin saturation. In practice, the arterial oxygen tension (P_aO) is assigned a value,[1] and a corresponding value of S_aO is determined from the oxygen-hemoglobin equilibrium curve (*OEC*), an operation that can be expressed in functional form as

$$S_aO = OEC(P_aO) \tag{B2}$$

Oxygen Delivery at Tissues

Oxygen transport at the tissue level is schematically represented in figure B-1. In the present model, the tissue of concern is taken to be the erythropoietin-producing cells known to be located primarily within the kidneys. It has been assumed that the oxygen sensor as well as sites of erythropoietin production are responsive to the mean oxygen tension of the kidneys. This assumption permits tissue oxygen tension to be derived from an oxygen balance using blood flows, arteriovenous oxygen concentrations, oxygen consumption, and transcapillary diffusion resistances common to the kidneys, which are considered to be a homogenous tissue.

[1]See table B-I for symbol definitions, units, and normal values.

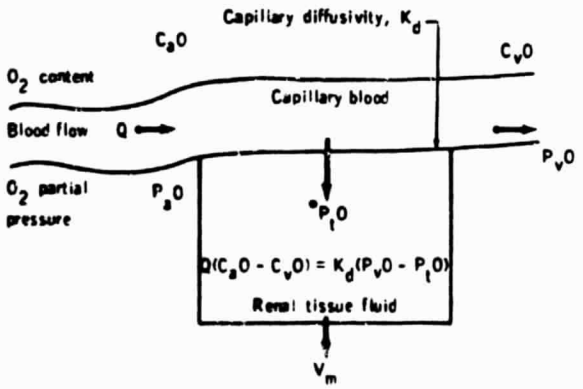

FIGURE B-1.—Two-compartment steady-state model of renal tissue oxygenation.

The elements of tissue oxygenation were determined using a two-phase model consisting of capillary blood and tissue fluid (ref. B-16). It is assumed that the blood compartment is well mixed with an oxygen partial pressure (P_vO) equal to that in the venous outflow. Oxygen diffuses from blood to tissue along a gradient of oxygen partial pressure ($P_vO - P_tO$), where P_tO is the oxygen tension of the homogenous tissue. The amount of oxygen unloaded from the blood is given by the difference in oxygen concentration between arterial and venous blood ($C_aO - C_vO$). At equilibrium, the rate of oxygen transfer to the tissues is identical to the tissue oxygen consumption (V_m) and to the unloading of blood oxygen as determined by the arteriovenous oxygen concentration. In other words,

$$\underbrace{Q \times (C_aO - C_vO)}_{\text{Rate of oxygen unloading}} = \underbrace{K_d \times (P_vO - P_tO)}_{\text{Rate of oxygen diffusion}} = V_m \tag{B3}$$

where Q is the rate of regional blood flow and K_d is the diffusive transfer coefficient between blood and tissue.

The venous partial pressure may be obtained by solving equation (B3) for C_vO

$$C_vO = C_aO - (V_m/Q) \tag{B4}$$

then computing venous hemoglobin saturation from a formulation analogous to equation (B1)

$$S_vO = C_vO/(Hct \times MCHC \times CHbO) \tag{B5}$$

and determining P_vO from the *OEC*, expressed in functional form as

$$P_vO = OEC(S_vO) \tag{B6}$$

Tissue oxygen tension can now be derived from equation (B3) as

$$P_tO = P_vO - V_m/K_d \tag{B7}$$

The assumption of steady state in this formulation implies rapid equilibration of oxygen in the fluid phase and is not meant to suggest a constant tissue oxygen tension during the simulation of an

erythropoietic disturbance. Since the erythropoietic process itself has been modeled dynamically, the hematocrit will be time-varying until red cell production achieves its own steady state. In this model, the hematocrit is a major influence on alterations in tissue oxygen tension. In addition, other quantities in this algorithm (P_aO, V_m, K_d, $P50$, Q) are nonregulatory parameters and can also influence tissue oxygen tension if they are manually altered.

Erythropoietin Production and Distribution

Erythropoietin release is assumed to be governed by the tissue oxygen tension. A limited number of studies (refs. B-5 and B-17 to B-19) suggest a relationship of the form[7]

$$\overline{E_p} = E_o \exp\left(-G_1 \overline{P_tO}\right) \qquad \text{(B8)}$$

where $\overline{E_p}$ is the rate of erythropoietin production, $\overline{P_tO}$ is the tissue oxygen partial pressure, G_1 is the gain or slope of the function plotted linearly as the natural log of $\overline{E_p}$ versus $\overline{P_tO}$, and E_o is the $\overline{E_p}$ intercept at $\overline{P_tO} = 0$. Setting $E_o = \exp(G_1)$ ensures that equation (B8) will always pass through the normal operating point ($\overline{E_p} = 1.0$, $\overline{P_tO} = 1.0$) irrespective of values of G_1. In certain cases, it may be desirable to postulate a shift in the normal operating point as well as gain, and in those cases, E_o and G_1 may be adjusted separately. Figure B-2 illustrates the semilogarithmic relationship between tissue oxygen tension and erythropoietin production and shows the influence of G_1.

The concentration of erythropoietin in the plasma (E) is a function of the rate of production (E_p), the rate of clearance or destruction (E_d), and the volume of distribution (V_e). If it is assumed that the rate of disappearance is proportional to the plasma concentration (i.e., $E_d = K_e \times V_e \times E$, where K_e = clearance constant = $\log_e 2$/plasma half-life), then the following first-order differential equation can be written for the rate of change of erythropoietin concentration (refs. B-8 and B-17):

$$\frac{dE}{dt} = \frac{E_p}{V_e} - K_e E \qquad \text{(B9)}$$

[7]The bar over the symbols represents normalized values. Thus, $\bar{X} = X/X(o)$, where $X(o)$ is the control or pretreatment condition and X is a value during the postcontrol or treatment phase. The use of normalized values simplified comparison of model response with data from various laboratories.

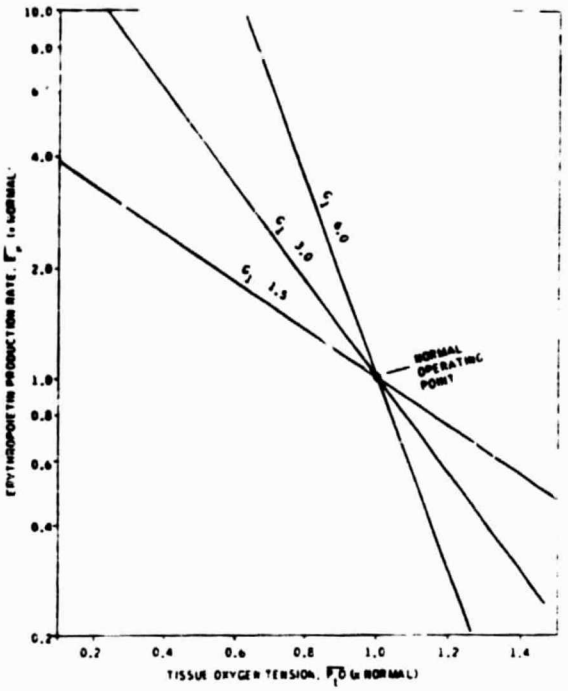

FIGURE B-2.—Renal controller function for erythropoietin production rate showing effect of gain G_1.

The steady-state concentration of E (at $dE/dt = 0$) is, therefore

$$E(o) = E_p(o)/K_e V_e \qquad \text{(B10)}$$

Equation (B9) can be normalized by letting $\bar{E} = E/E(o)$ and $\overline{E_p} = E_p/E_p(o)$ and substituting equation (B1) into equation (B9):

$$\frac{d\bar{E}}{dt} = K_e\left(\overline{E_p} - \bar{E}\right)$$

$$= \frac{\log_e 2}{TE_{1/2}}\left(\overline{E_p} - \bar{E}\right) \qquad \text{(B11)}$$

a form that has the advantage of being independent of distribution volume and, further, independent of erythropoietin half-life ($TE_{1/2}$) at steady state, since $\bar{E}(o) = \overline{E_p}(o)$. The value of $TE_{1/2} = 12$ hours was chosen for humans, but this does not appear to be well established for normal subjects (ref. B-20).

Red Blood Cell Production

An equation expressing the semilogarithmic dose-response relationship between red cell pro-

duction (RCP) and erythropoietin concentration (E) can be given as

$$\overline{RCP} = G_2 \log_e \bar{E} + P_1 \qquad \text{(B12)}$$

As has been the convention, RCP and E have been normalized with respect to their steady-state control values, G_2 is the gain or slope of the response curve, and P_1 is the value of $\overline{RCP}$ when $\bar{E} = 1.0$ and is normally taken as unity.

The accuracy of equation (B12) may diminish considerably at very low and very high values of erythropoietin levels. For example, at decreasing values of $\bar{E}$ approaching zero, the production rate tends toward minus infinity rather than zero, whereas at high $\bar{E}$ values, the relationship does not exhibit a maximal production that is known to exist. Therefore, two additional equations were formulated and piecewise fitted to equation (B12) to account for suppressed and maximal erythropoiesis. (See fig. B-3.) Their precise description is somewhat speculative, although this bone marrow function curve closely corresponds to the sigmoid shape of most biological dose-response relationships (ref. B-21) and to those observed by others for the bone marrow (refs. B-22 to B-24).

In the present study, it was assumed that there is no basal production of red cells unless erythropoietin is present (i.e., $P_0 = 0$). Maximal red cell production is assumed to be six times normal (ref. B-17) ($P_m = 6$) and the upper limit of accuracy of equation (B12) was arbitrarily chosen at $\overline{RCP} = 5$.

Iron uptake studies of red cells indicate a bone marrow transit time for red cell production of 3.5 to 4.5 days (ref. B-10). This effect was included in the model using a simple first-order time delay[3] with a time constant T_{BM}. The inclusion of this transit delay clearly improved the realism of the dynamic response of the model, especially following sudden changes in tissue oxygen tension.

Red Cell Destruction and Red Cell Mass

The lifespan of the red cell dictates the destruction rate of cells. A model of red cell destruction was assumed in which cells are destroyed randomly and no cells survive past a given lifespan (ref. B-25). In that case, the rate of destruction (RCD) is simply proportional to the amount of cells present at any time. If that amount is given as RCM, then the rate of red blood cell destruction will be

$$RCD = K_r \cdot RCM$$

$$= \log_e 2 \cdot RCM / TRC_{1/2} \qquad \text{(B13)}$$

where $TRC_{1/2}$ = red cell half-life and K_r = red cell clearance constant = $\log_e 2 / TRC_{1/2}$. At normal values used in the model, the rate of red cell destruction is 1.1 percent of the total amount present or 22 ml of packed cells/day.

The instantaneous change in total circulating red cell mass is the net difference between red cell production and red cell destruction rates:

$$\frac{d(RCM)}{dt} = RCP - RCD \qquad \text{(B14)}$$

The quantity RCP is obtained from equation (B12) using the transformation $RCP = \overline{RCP} \times RCP(o)$, where $RCP(o) = RCD(o) = K_r \cdot RCM(o)$.

Finally, the current value of RCM, obtained by integration of equation (B14), is combined with the plasma volume to obtain the whole-body hematocrit of the circulation:

$$Hct = \frac{RCM}{PV + RCM} \qquad \text{(B15)}$$

and the feedback loop is closed.

The Renal/Bone-Marrow Axis as a Proportional Controller

A more visual understanding of the relationships for renal and bone marrow function can be obtained by determining the overall dose-response curve of the combined kidney/bone-marrow axis; that is, the relationship between tissue oxygen tension and red cell production. The results are shown here only for the midrange of erythropoietin production and were obtained by mathematically combining the renal function (eq. (B9)) with the steady-state plasma distribution function of erythropoietin (eq. (B11); $\bar{E} = \bar{E}_p$) and the bone marrow function (eq. (B12)). In this way,

[3] If Y is the steady-state value predicted from a dose-response relationship, then the response delayed with a time constant T is obtained by the solution of the differential equation $T\,dy/dt + y = Y$. In finite difference form, suitable for iterative computer solution, this becomes $y_i = y_i + (Y - y_i)(H/T)$ where H = integration step size, y_i = value of y at the ith iteration, and y_i = value of y at the $i+1$th iteration

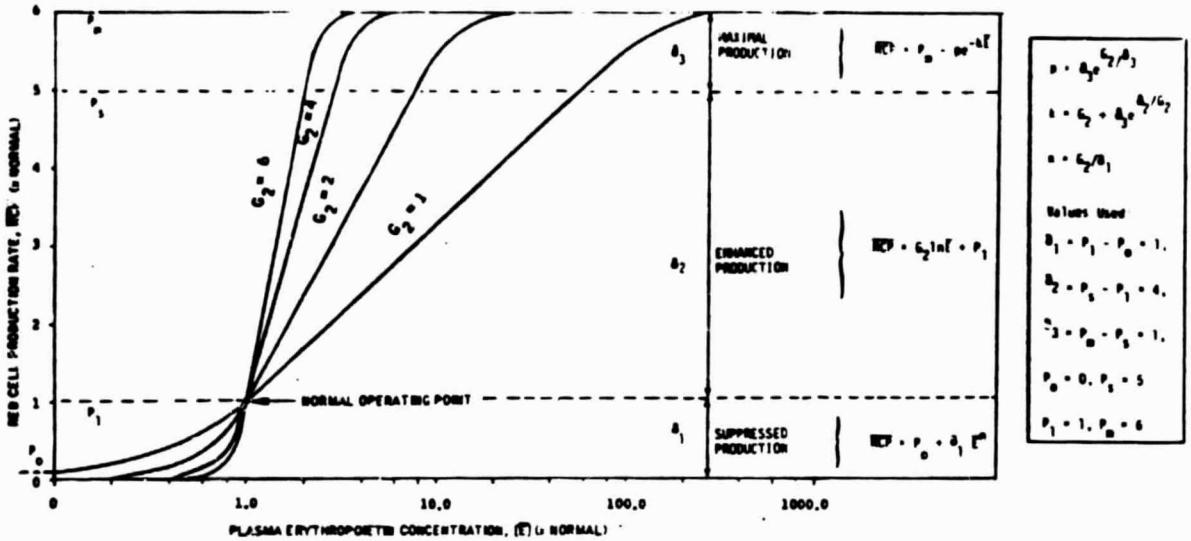

FIGURE B-3.—Bone marrow controller function for red cell production rate showing equations used to piecewise fit the dose-response curve and demonstrating effect of gain G_1.

erythropoietin is eliminated as an explicit variable; i.e.,

$$\overline{RCP} = G\left(1 - \overline{P_tO}\right) \quad \left(\text{for } \overline{P_tO} < 1\right) \quad \text{(B16)}$$

where $G = G_1 \times G_2$. This is a simple inverse linear relationship that has previously been used in the models of Guyton et al. (ref. B-15) and Hodgson (ref. B-5). In this form, the gain of the renal/bone-marrow (open loop) system is seen to be the product of the two gain factors, G_1 and G_2. Similar (although nonlinear) gain-product relationships were obtained for the extreme of hyperoxia and maximal hypoxia. The results of this analysis have been plotted in figure B-4 for a range of values of G. This function represents the entire controller circuit of the erythropoiesis model. In general, hypoxic tissue is predicted to have a greater effect on red cell production than hyperoxic tissue, as indicated by the relative slopes. However, at higher gain factors, the suppression of erythropoiesis can be considerable for relatively small increases in tissue oxygenation.

Equation (B16) is a typical controller function for a linear proportional control system in which the actuating error signal is the deviation of $\overline{P_tO}$ from its control value (unity) and G is the constant of proportionality or controller gain. The control value of $\overline{P_tO}$ is taken as an arbitrary reference standard and is not meant to imply that there is an internal set-point. It becomes clear from this control function that the primary controlled variable is tissue oxygen tension rather than red cell production, red cell mass, or hematocrit, which can be considered controller variables. The control system always adjusts the controller variables in a direction that returns the controlled variable toward normal after an initial load disturbance. (See fig. A-1 in app. A.)

The controller gain is a major determinant of the final feedback compensation following a disturbance and, within limits, the speed at which a disturbance is corrected. Although increasing the gain increases the feedback effect, it may be at the sacrifice of an oscillatory approach to the steady state. Systems of higher order than this one will tend to become unstable as controller gain increases. Oscillations in the erythropoiesis system are known to occur in special cases, and analysis of these systems in terms of control system theory has proved to be rewarding (refs. B-26 and B-27).

Model Operation

The system of equations (B1), (B2), (B4) to (B8), and (B11) to (B15) is solved by computer simulation using an iterative procedure. Equations (B11) and (B14) are integrated numerically using a simple Euler algorithm (ref. B-28) and initial conditions $E(o)$ and $RCM(o)$, respectively. The program is currently implemented on a Univac 1110 and a

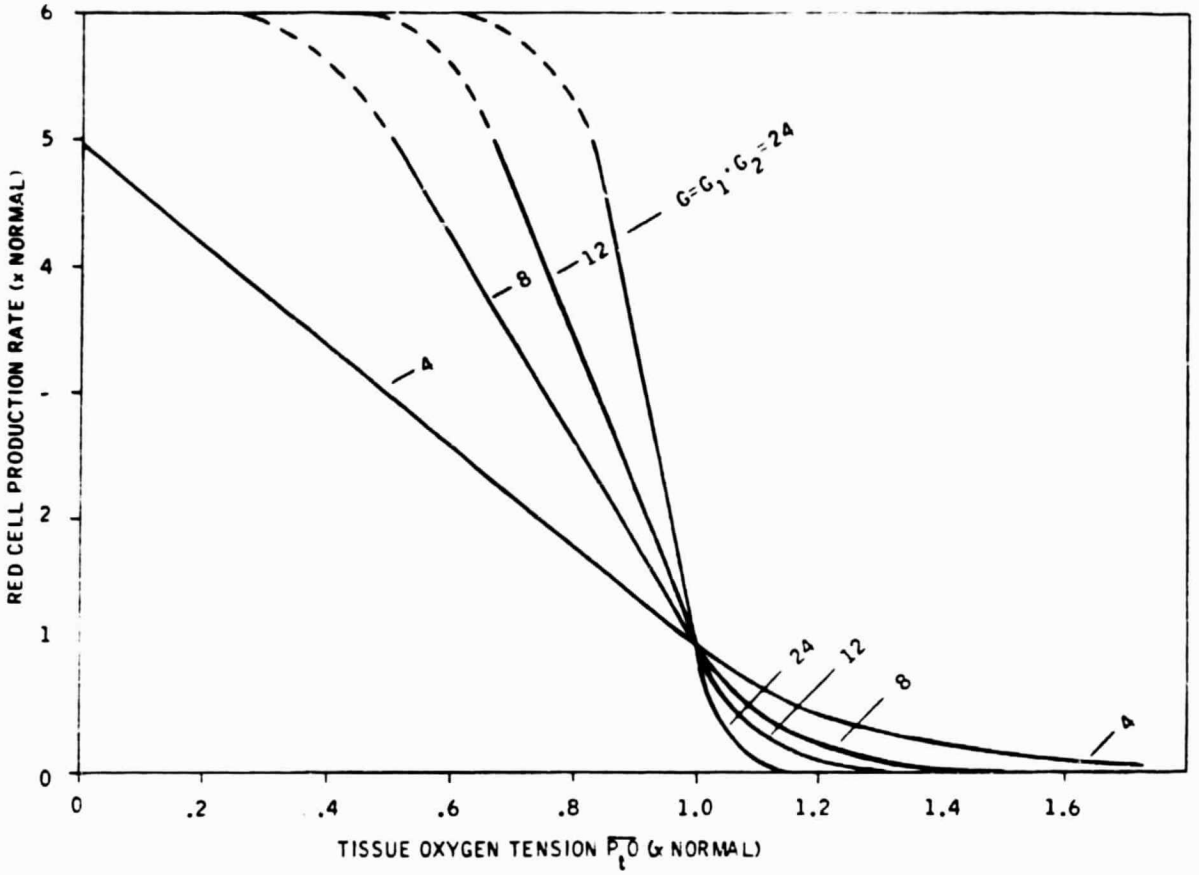

FIGURE B-4.—Combined renal/bone-marrow controller function showing effect of tissue oxygen tension on erythropoiesis for various values of overall gain *G*.

PDP 11/40 using Fortran language. Remote terminals including graphic display of the simulation responses (and experimental data simultaneously, when desired) have greatly facilitated user interaction and have enhanced the convenience of model validation.

Perturbing the model away from its normal steady state (initial conditions) is accomplished by altering one of the model parameters.[4] These quantities are normally constant in value but can be altered during a run to simulate either independent stress stimuli or long-term regulatory adjustments. Thus, hypoxia may be simulated by decreasing arterial oxygen partial pressure (pO_2), and hemolysis may be simulated by decreasing the red cell lifespan. In some cases, alteration of more than one parameter may be desired as in the simulation of altitude hypoxia which involves a primary change in arterial pO_2 and a compensatory shift in oxygen-hemoglobin affinity (*P*50). Parameter values may be time-invariant with values fixed before a simulation run or they may be entered as a function that varies with time as the run progresses. Experimental data may be used to drive the model in this fashion. Thus, it is possible to simulate a wide variety of stresses and to test a large number of hypotheses regarding regulating mechanisms.

[4]The term "parameter" is used to denote time-invariant quantities that are not altered by the dynamic properties of the model as opposed to "dependent variables" that are time-varying and form the connecting links of the feedback circuit (i.e., P_tO, *E*, *RCP*, *Hct*, etc.)

Parameter Estimation

Table B-I lists the values of the system parameters, chosen as representative of the human system. Also shown are the steady-state control

TABLE B-I.—Parameters and Initial Conditions

Symbol	Definition	Value	Units
	Parameters		
$CHbO$	Carrying capacity of hemoglobin	1.34	ml O_2/g Hb
E_o	Intercept of erythropoietin function	20.09	× normal
G_1	Gain of erythropoietin function	3	Nondimensional
G_2	Gain of red cell production function	2	Nondimensional
K_d	Capillary diffusivity	.567	ml O_2 min^{-1} $mmHg^{-1}$
		4.25	ml O_2 min^{-1} kPa^{-1}
$MCHC$	Mean corpuscular hemoglobin concentration	.375	g Hb/ml RBC
P_aO	Oxygen tension in arterial blood	95.0	mmHg
		12.67	kPa
PV	Plasma volume	3.0	Liters
P_m	Maximum production rate of red cells	6	× normal
P_o	Minimum production rate of red cells	0	× normal
P_1	Normal production rate of red cells	1	× normal
$P50$	Oxygen tension of hemoglobin at 50 percent saturation	26.7	mmHg
		3.56	kPa
Q	Renal blood flow	1.2	Liters/min
TBM	Bone marrow transit time	4	Days
$TE_{1/2}$	Plasma half-life of erythropoietin	12	Hours
$TRC_{1/2}$	Red cell half-life	63	Days
V_m	Oxygen uptake of kidneys	20	ml O_2/min
	Initial conditions		
C_aO	Oxygen content of arterial blood	19.6	ml O_2/100 ml blood
C_vO	Oxygen content of venous blood	17.9	ml O_2/100 ml blood
$\overline{E}$	Erythropoietin concentration in plasma	1.0	× normal
$\overline{E_p}$	Erythropoietin production rate	1.0	× normal
Hct	Hematocrit	40	ml of packed RBC/100 ml blood
P_tO	Oxygen tension in renal tissue fluid	20	mmHg
		2.67	kPa
P_vO	Oxygen tension in venous blood	55.3	mmHg
		7.37	kPa
RCM	Red cell mass	2.0	Liters
RCP	Production rate of new red blood cells		ml of packed cells/day
S_aO	Saturation of arterial hemoglobin with oxygen	97.6	Percent
S_vO	Saturation of venous hemoglobin with oxygen	89.3	Percent

values (i.e., initial conditions) of the major dependent (output) variables. The precise values of most of the quantities shown in table B-I are not critical, however, to the general behavior of the model's response when expressed in percent deviation from control. An exception to this occurs for the highly nonlinear functions such as the oxygen equilibrium curves and the renal and bone marrow function curves. The location of the operating point on these curves can change the nature of the output response. Also, the shapes of these curves, as defined by the gains and threshold parameters, are critical to the magnitude of the response. These will be discussed next.

An equation for the oxygen equilibrium curve was obtained from Aberman et al. (ref. B-29). Their study included a computer algorithm that converts oxygen tension to saturation and, with iteration, oxygen saturation to tension. The agreement between measured and computed values is claimed to be better than 0.2 percent. In addition, the algorithm includes the capability of altering $P50$ values. (See fig. B-5.)

Analysis of Adamson's data (ref. B-18), from which the erythropoietin release function was obtained, leads to an estimated value of $G_1 = 2.8$. In

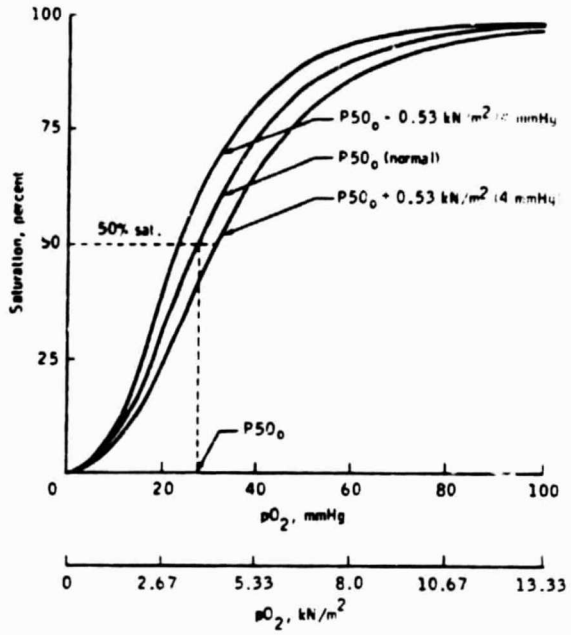

FIGURE B-5.—Oxygen-hemoglobin equilibrium curves drawn directly from computer model output showing effect of changing the *P*50 parameter. The *P*50 value is the oxygen tension at which 50 percent of the hemoglobin is saturated and is, therefore, an index of oxyhemoglobin affinity. The position of the OEC may vary in accordance with known effects of hydrogen ion, CO_2, temperature, or 2,3-DPG (diphosphoglycerate). The effects of DPG are of interest because of its possible contribution to erythrokinetic changes during bed rest or weightlessness.

simulation studies of bed rest and hypoxia (refs. B-30 and B-31), values of G_i were determined by parameter estimation to range from 2 to 5. No data exist to confirm these estimates directly. It is permissible to use the gain factors as adjustable parameters, within reasonable limits, in order to test hypotheses and possibly provide improved agreement between model and experiment data. In addition to the gains or sensitivities, the other parameters of these functions (E_0, P_0, P_1) that can be thought of as threshold indices are also not well known and are available for parameter estimation during a simulation. Changing these latter quantities implies a shift of the normal operating points ($\overline{E_p} = 1$, $\overline{P_tO} = 1$) for fig. B-2; ($\overline{RCP} = 1$, $\overline{E} = 1$) for fig. B-3). The value of K_d was obtained from equation (B7) by dividing the oxygen uptake by $P_vO - P_tO$. The value of P_tO was arbitrarily assumed to be 2.67 kN/m² (20 mmHg), and P_vO was computed from equations (B1), (B2), and (B4) to (B6).

Steady-State Errors

It is an inherent property of most biological homeostatic mechanisms in general and proportional control systems in particular that there will be at least some residual steady-state deviation from the normal operating point when the system is disturbed by a constant load. This "steady-state error" will vary in size depending on the gain of the system and the magnitude of the load disturbance. The sensitivity coefficients of table III-6, for example, indicate the steady-state errors of red cell production resulting from small changes in parameter disturbances.

A basis for understanding steady-state errors in the current model is as follows. At any equilibrium state, the term *dRCM/dt* in equation (B14) must be identically zero. Therefore, equations (B13) and (B14) imply that, at steady state, daily red cell production and destruction rates are equal. Furthermore, if red cell lifespan is constant, a steady-state alteration in red cell mass implies a proportionate change in red cell production. Most load disturbances are accompanied by changes in circulating red cell mass (fig. B-1). This implies that red cell production and one or more of the factors that affect red cell production (including tissue oxygen tension, erythropoietin, hematocrit, controller gain, and set-point) must have incurred a steady-state error, however small. It can be appreciated from figure B-1 that steady-state errors in tissue oxygen tension are reduced at the expense of larger errors in red cell mass and hematocrit.

Steady-state analysis may also provide insight into the independent determinants of the controlled variable (ref. B-32). Figure B-6(a) shows the effect of tissue oxygen tension on red cell production (the controller function of fig. B-4) and the balance between red cell production and destruction. Feedback control ensures that the various elements of the model are adjusted until the rate of red cell mass change, *dRCM/dt*, becomes zero and that steady state is defined by this condition. It is mathematically permissible to set *dRCM/dt* to equal zero and work backward from this point to visualize those factors that determine tissue oxygen tension (fig. B-6(b)) There are only two such factors in our model: red cell destruction (which determines production rate) and the relationship between tissue oxygen tension and red cell production. Only these factors and those quantities that affect these factors will ultimately determine tissue oxygen tension.

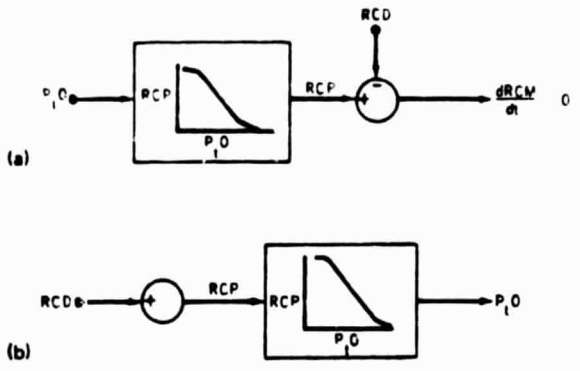

FIGURE B-6.—Steady-state analysis of long-term determinants of tissue oxygen tension. (a) Segment of feedback circuit that results in the term *dRCM/dt* becoming zero at steady state when destruction and production rates are equal. (b) Reversal of diagram in figure B-6(a) starting from the zero point and showing mathematically equivalent influences on tissue oxygen tension.

Experimental evidence is severely lacking on the determinants of the shape of the controller function curve, although it appears that it may be under the influence of neural and biochemical factors. (See subsection entitled "Discussion.") The factors that are responsible for normal red cell destruction are also not apparent (ref. B-10). Except for overt pathology, rates of destruction are generally considered to be a constant fraction of total circulating red cell mass.

Aside from these experimental shortcomings, it is important to note that the factors usually agreed to play a role in acute changes of tissue oxygenation (i.e., blood flow, capillary diffusivity, oxygen uptake, *P*50, hematocrit) are not represented between the zero point and the tissue oxygen point in figure B-6. Although they may be considered dependent variables in the system, none of them, from a mathematical point of view, are independent determinants of the *final* level at which the tissue oxygen tension will stabilize in the steady state. Although *dRCM/dt* will always return to its initial zero value, the tissue oxygen tension may exhibit a steady-state error due to the inherent properties of the control system in the face of a constant disturbance. However, based on the preceding analysis, the authors believe that even tissue oxygen tension will return to its initial value (zero steady-state error) when both of the following conditions are satisfied: (1) a constant daily rate of red cell destruction and (2) a constant controller relationship between tissue oxygen tension and red cell production.

As an example of the last point, a simulation of hypoxia was performed (fig. B-7) in which arterial oxygen tension was set at some low value for the entire run and red cell destruction was clamped at its control value of 22 ml of packed cells/day. Tissue oxygen tension decreased and then began to return toward normal as red cell production and hematocrit rose, similar to the simulations with the intact system shown in figure B-7(a). However, since the destruction rate was not permitted to increase, a greater net rate of red cells entered the circulation than would have occurred had destruction rate rose in accord with the mass action law of equation (B13). As a result, tissue oxygen tension continued to rise and red cell production rates declined. When the system reached its new steady state, red cell production and tissue oxygen tension returned exactly to the prehypoxic control conditions in accord with the concepts discussed in the previous paragraph. This was despite an arterial oxygen tension that was still significantly depressed and at the expense of hematocrit and circulating red cell mass that were considerably above normal.

It is perhaps easy to visualize that a primary change in destruction rate, as in hemolytic anemia, leads to secondary changes in tissue oxygen tension. It is more difficult to conceive of destruction rate being a determining factor of tissue oxygenation in a stress like hypoxia in which it appears, at first, that the decreased oxygen loading of arterial hemoglobin is the primary stimulus for hypoxia. However, it is important to distinguish between the initial stimulus of the acute phase, which blood pO_2 is controlling, and the ultimate stimulus of the steady-state condition, which destruction rate (and controller function) is controlling. These conclusions from a theoretical model may warrant further experimental examination. The simulation of hemolytic anemia presented in Section VIII illustrates the capability of the control system to minimize steady-state errors.

DISCUSSION

Renal pO_2 Sensor

A major assumption in the controlled system is the description of the renal oxygen detector. The evidence strongly indicates that the balance be-

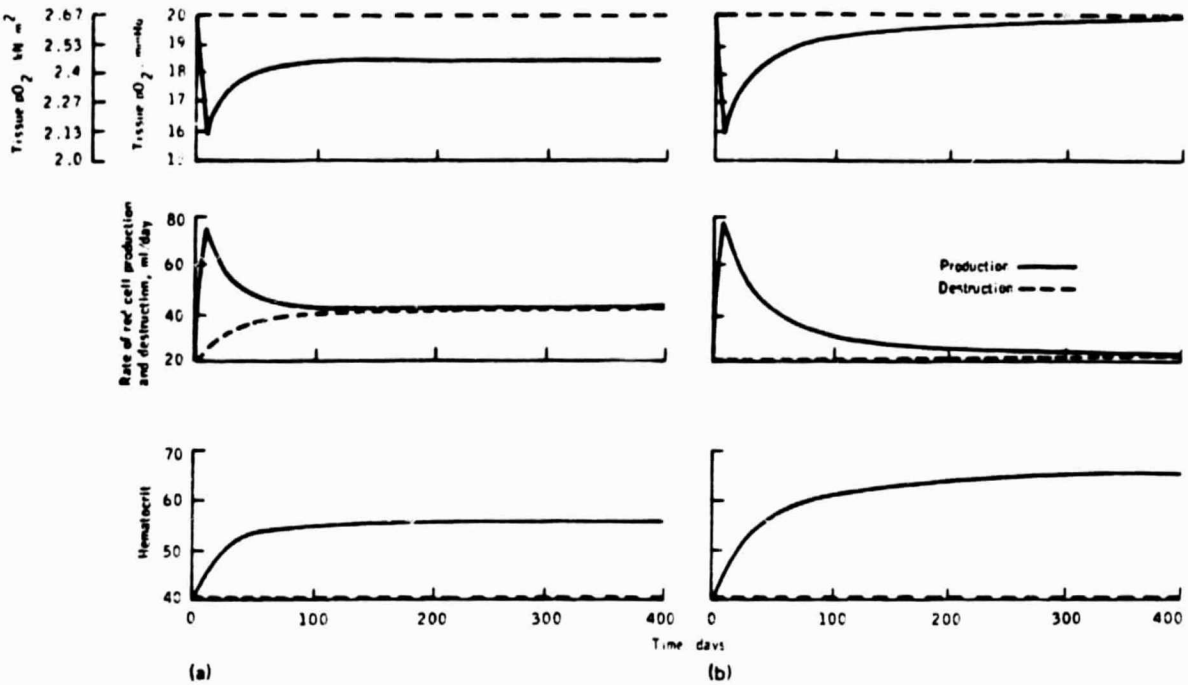

FIGURE B-7.—Effect of destruction rate on long-term control of tissue oxygen tension. (a) Normal simulation response to hypoxic stress. (b) Hypoxic simulation with destruction rate clamped at control value and showing regulation of tissue pO_2 back to normal despite reduced P_aO.

tween oxygen supply and demand at intrarenal sites is the primary stimulus for erythropoietin release (refs. B-7 and B-33). Furthermore, these detector sites must monitor venous or tissue pO_2 rather than arterial pO_2 since anemia or increased oxygen-hemoglobin affinity lead to increased erythropoietin production without significantly altering arterial blood oxygen tension (refs. B-5, B-34, and B-35). The receptors sensitive to tissue pO_2 may be those cells that excrete erythropoietin or its precursor (ref. B-13). The present model is in accord with these concepts.

It has been suggested that the kidney has unique characteristics that enable it to function as a sensitive oxygen chemoreceptor and, in particular, be responsive to changing hemoglobin levels. The peculiar renal microcirculation and the uniquely low arteriovenous oxygen difference provide a gradient of tissue oxygen tension that amplifies changes in blood oxygen delivery (refs. B-14 and B-35). In addition, the autoregulatory features of the kidney ensure that blood flow and oxygen uptake are effectively stable over a wide range of oxygen tensions and blood pressures (refs. B-36 and B-37). Moreover, if blood flows should be altered, the kidney, in contrast to other organs, will exhibit proportionate changes in oxygen uptake (ref. B-38). This means that the ratio V_m/Q (the only term in which blood flow appears in the model (eq. (B4)) may be relatively constant, and renal blood flow would not be expected to markedly influence tissue oxygenation.

The preceding discussion suggests that the powerful influence which oxygen uptake, per se, was found to have in the model (fig. B-1 and table B-I) may be mitigated in the real system by concurrent changes in blood flow. Similarly, it is possible that an elevation of V_m, by whatever cause, promotes tissue hypoxia and results in local regulatory increases of K_d, the effective capillary diffusivity. This is now known to be true for skeletal muscle (ref. B-39) but has not been confirmed for the kidney. Such regulation would, however, further dampen the effect of oxygen uptake because K_d appears only in the ratio V_m/K_d in equation (B7). It may be desirable to add these local regulatory effects—between oxygen uptake, blood flow, and capillary diffusivity—to the model. A current alternate approach is to assume they are constant and to examine their influence, if the data so suggest, in

improving the accuracy of simulation. Under these circumstances, and in accord with equations (B1) to (B7), tissue pO_2 would be a function of the hemoglobin concentration of the blood, the arterial oxygen saturation of hemoglobin, and the shape and position of the OEC (ref. B-6).

It should be emphasized that the site of the intrarenal detector has not yet been confirmed and that the quantitative aspects of its oxygen supply-demand balance (including direct measurement of P_tO) remain unknown. Justification of this segment of the model is based on indirect evidence, gross characteristics of the kidney as a whole, and determinants of tissue oxygenation derived from other tissues.

The use of a steady-state formulation for tissue oxygenation (eqs. (B1) to (B7)) in a dynamic model is justified because, in the well-perfused kidney, equilibrium of oxygen tension due to pure convection and diffusion may be achieved in the order of seconds to minutes following a load disturbance. This can be compared to the much slower changes of the erythropoietin distribution or bone marrow red cell production process. Estimates of true equilibration times were obtained from the non-steady-state version of this algorithm (refs. B-16 and B-40) that was originally employed in the NASA studies. The steady-state description permitted the use of a larger integration step size in the numerical algorithms and increased the solution speed significantly without decreasing the accuracy of the response for the long periods of time in which the investigators were interested.

Bone Marrow Controller System

An accurate description of the relationship governing erythropoietin release is not yet available, presumably because of the difficulty in measuring intrarenal oxygen levels and the uncertainty surrounding the specific location of the receptor cells. The formulation used to relate tissue oxygen tension to erythropoietin release is in accord with the study of Adamson (ref. B-18), who found a semilogarithmic inverse relationship between daily urinary erythropoietin excretion and hematocrit in humans. A parallel between urinary and plasma erythropoietin (ref. B-7) as well as between hematocrit and tissue pO_2 (ref. B-41) was assumed in deriving equation (B8). A similar relationship has been used by Hodgson (ref. B-5), whereas Parer (ref. B-42) has derived a linear relationship and Mylrea and Abbrecht (ref. B-17) have used arterial oxygen-hemoglobin concentration (i.e., $Hb \times S_aO$) rather than tissue oxygen tension as the independent variable. At the present time, sufficient data do not exist to reveal the precise shape of this function.

Measurement of plasma erythropoietin has, until recently, been restricted to levels above basal (ref. B-1). Therefore, no data are available to confirm the relationship to reduced release rates of erythropoietin. This region is of particular interest because of its application of simulation to bed rest, space flight, and related disturbances in which chronic elevation of hematocrit follows plasma volume shifts.

There is an abundance of information demonstrating that in experimental animals, a linear relationship exists between red cell production and the log of erythropoietin concentration (eq. (B12)). This has been observed, for example, in bioassay animals in which doses of erythropoietin are injected either singularly with iron uptake used as the index of erythropoietic activity (refs. B-2 and B-24) or administered at frequent intervals for up to several weeks with production rate expressed in terms of increased red cell mass (refs. B-9 and B-23). It is reasonable to assume that a similar dose-response relationship exists for the human, although confirmatory evidence is lacking. In vivo estimates of the human function curve, especially for the suppressed erythropoiesis range, will be possible as erythropoietin becomes available in large quantities and as more sensitive assay methods for this hormone are developed.

The shape and position of the renal and bone marrow function curves have been found to be crucial elements in the control of erythropoiesis in general and in the long-term control of tissue oxygenation in particular. Model parameters have been incorporated to allow for shifts in sensitivities and thresholds away from the normal operating points. Values of controller sensitivities have not been well established in the human by direct methods and only to a limited extent in experimental animals (ref. B-5). Several studies suggest that alterations in these parameters occur during certain physiological stresses such as dehydration and hypoxia (refs. B-43 and B-44) and during pathological disturbances such as abnormal hemoglobin (ref. B-34), erythrocytosis (ref. B-18), and hemolytic anemia (ref. B-45). It appears that the rate of red

cell production is determined not only by the concentration of erythropoietin but also by the size of the stem cell pool (ref. B-46). If this is true, the bone marrow response to a given dose of erythropoietin should be greater than normal (i.e., an effective increase in G_2). The availability of iron to the erythron may also influence this function (ref. B-11). Certain hormones, such as androgens, as well as neural stimuli are assumed to exert their effect on erythropoiesis by their modification of erythropoietin release (i.e., an effective change in G_1; refs. B-12 and B-13). It is possible, using the current model, to predict these parameters within narrow limits provided both the dynamic behavior of erythropoietin and red cell production ates are measured simultaneously during hematologic stress. Unfortunately, such data are seldom available, especially for humans.

General Comments

Feedback regulation of tissue oxygen tension is accomplished solely by adjustments of hemoglobin levels resulting from the output of a renal/bone-marrow controller. Other parameters that are known to effect acute changes in tissue oxygenation are incorporated explicitly in the model but are nonregulatory in nature and can be altered manually to test various hypotheses. Similarly, the characteristics of the controller can also be adjusted to test their effect on long-term control of tissue pO_2 and red cell mass. Such parameter adjustment (other than for the primary disturbance) has not been found to be essential, in most cases, to simulate the basic behavior of the dynamic and steady-state response. However, fine tuning of parameters is required to scale the model output and achieve closer agreement with experimental values. In some cases, these studies indicate the need to propose additional regulatory elements to provide, for example, a more realistic simulation of the erythropoietin response to hypoxia. Other features of a general nature have also been identified that will increase the utility of the model even further, including (1) the effect of blood volume and viscosity on oxygen transport and (2) a description of stem cell kinetics and reticulocytosis (ref. B-47).

FORMULATION OF MOUSE MODEL

System Parameters

The computer model for erythropoietic control was adapted to the mouse system by altering system parameters originally given for the human to those that more realistically represent the mouse (ref. B-48). Parameter values were obtained from a variety of literature sources as indicated in table B-II. The immediate application of the mouse model was the study of the mouse as a potential experimental model for space flight. Data for the simulations were obtained from C. D. R. Dunn's experiments at the University of Tennessee Memorial Research Center and included studies of dehydration and hypoxia. The strain of mice used in these studies was C3H with an approximate weight of 25 grams. Parameter values were chosen for this strain where possible. In certain cases, the literature values were superseded by values obtained directly from Dunn's studies. In a few cases, mouse data were not available and data for the rat were substituted. A comparison of system parameters for the mouse and human models is shown in table B-II. Aside from the obvious differences expected in fluid volumes, blood flows, and metabolic rates, larger differences were observed in the following: erythrocyte lifespan (126 days vs. 20 days),[5] erythropoietin half-life (12 hours vs. 3.25 hours), and normal arterial pO_2 (12.67 kN/m^2 (95 mmHg) vs. 10.4 kN/m^2 (78 mmHg)). The shorter lifespan of the mouse red blood cells implies a turnover of erythrocytes which is sixfold faster. That is, the daily rates of red cell production and destruction (as well as reticulocyte index) are approximately six times higher in the C3H mouse than the human.[6] Other parameters which were found to be more similar between the two species were as follows: hematocrit (40 vs. 45), mean corpuscular hemoglobin concentration (0.375 vs. 0.30), and maximum oxygen-carrying capacity of hemoglobin (1.34 vs. 1.41).

[5]First and second numbers in parentheses refer to human and mouse, respectively.

[6]Typical values for mice red cell lifespan found in the literature indicate only a threefold increase. Values used here were found by Dunn to be much different in the C3H strain.

TABLE B-II.—System Parameters for Erythropoiesis Control Model

Parameter	Model symbol	Parameter value		Reference	Units
		Human	Mouse		
Red cell mass[a]	*RCM*	2000	0.63	B-49	ml
Plasma volume[a]	*PV*	3000	.77	B-49	ml
Blood volume	*BV*	5000	1.40	B-49	ml
Whole-body hematocrit	*Hct*	40.0	45.0	B-49	ml of packed RBC/100 ml blood
Mean corpuscular hemoglobin concentration[a]	*MCHC*	.375	.300	B-50	g Hb/ml RBC
Hemoglobin concentration[a]	*Hb*	15.0	13.5	B-50, B-51	g Hb/100 ml blood
O_2 capacity of blood[a]	C_aO	20.1	19.0	B-51	ml O_2/100 ml blood
O_2 capacity of hemoglobin	*CHbO*	1.34	1.41	B-50, B-51	ml O_2/g Hb
pO_2 tension at one-half Hb saturation[a]	*P50*	27	39	B-52	mmHg
		3.6	5.2		kPa
[a]Arterial pO_2	P_aO	95	78	B-53	mmHg
		12.67	10.4		kPa
Arterial Hb saturation	S_aO	.97	.99	B-52	Percent
Renal metabolic rate[a]	V_m	20	.04	B-54	ml O_2/min
Renal blood flow[a]	*Q*	1200	1.83	B-55	ml/min
[a]Normal tissue pO_2	*P.O*	20	20		mmHg
		2.67	2.67		kPa
Erythropoietin half-life[a]	$TE_{1/2}$	12	3.25	B-56	Hours
Red cell lifespan[a]	*TRC*	126	20	B-17	Days
Erythrocyte maturation time[a]	*TBM*	4	3.5		Days
Normal RBC production rate[a]	*RCP*	22	.0437	B-49	ml RBC/day
RBC turnover rate	*RAC*	1.1	6.93	B-49	Percent/day

[a]Fundamental value from which other parameter values may be derived. Relationships used in deriving these other parameters are as follows:
Blood volume: $BV = RCM + PV = 0.63 + 0.77 = 1.4$ ml
Whole-body hematocrit: $Hct = RCM/BV = 0.63/1.4 = 0.45$ ml packed RBC/ml blood
Hemoglobin concentration: $Hb = Hct \times MCHC = 45 \times 0.3 = 13.5$ g Hb/100 ml blood
Capacity of hemoglobin: $CHbO = C_aO/Hb = 19.0/13.5 = 1.41$ ml O_2/g Hb
Arterial Hb saturation: S_aO = function (P_aO) (See oxygen-hemoglobin dissociation curve (fig. B-8).)
RBC turnover: RAC = turnover rate. $100 = 0.693$/RBC half-life $= 0.693/20.2 = 0.0693$ per day $= 6.93$ percent per day
Steady-state destruction rate: $RCM \times RAC = 0.63 \times 0.0693 = 0.0437$ ml/day

Although the arterial pO_2 in the mouse is much lower than in the human, the oxygen saturation of hemoglobin of both species is nearly identical (97 percent vs. 99 percent). This is a result of the distinctly different oxygen-hemoglobin dissociation curves shown in figure B-8 and reflected in the different *P*50 values (3.53 kN/m² (26.5 mmHg) vs. 5.2 kN/m² (39.0 mmHg)). The *P*50 differences imply that, at the same level of tissue oxygen tension, oxygen is more easily unloaded in the mouse than in the human. It should be noted that the normal pO_2 of arterial blood assumed here (10.4 kN/m² (78 mmHg)) was obtained from rat data (refs. B-51 and B-56) and has been used in a previous model validated for the mouse with reasonably good results (ref. B-17). No corresponding mouse data could be located.

Values for renal blood flow of the mouse were not available, and data from rats were used (6 ml min^{-1} g^{-1} tissue).

Scaled Parameters

Some parameters of the mouse model differ considerably from the human model because of scaling factors alone. The values used in the model are given on an absolute basis for the whole animal rather than as a specific property in terms of "per gram of tissue." In terms of specific units, the differences between the mouse and human system are much smaller, as shown in table B-III.

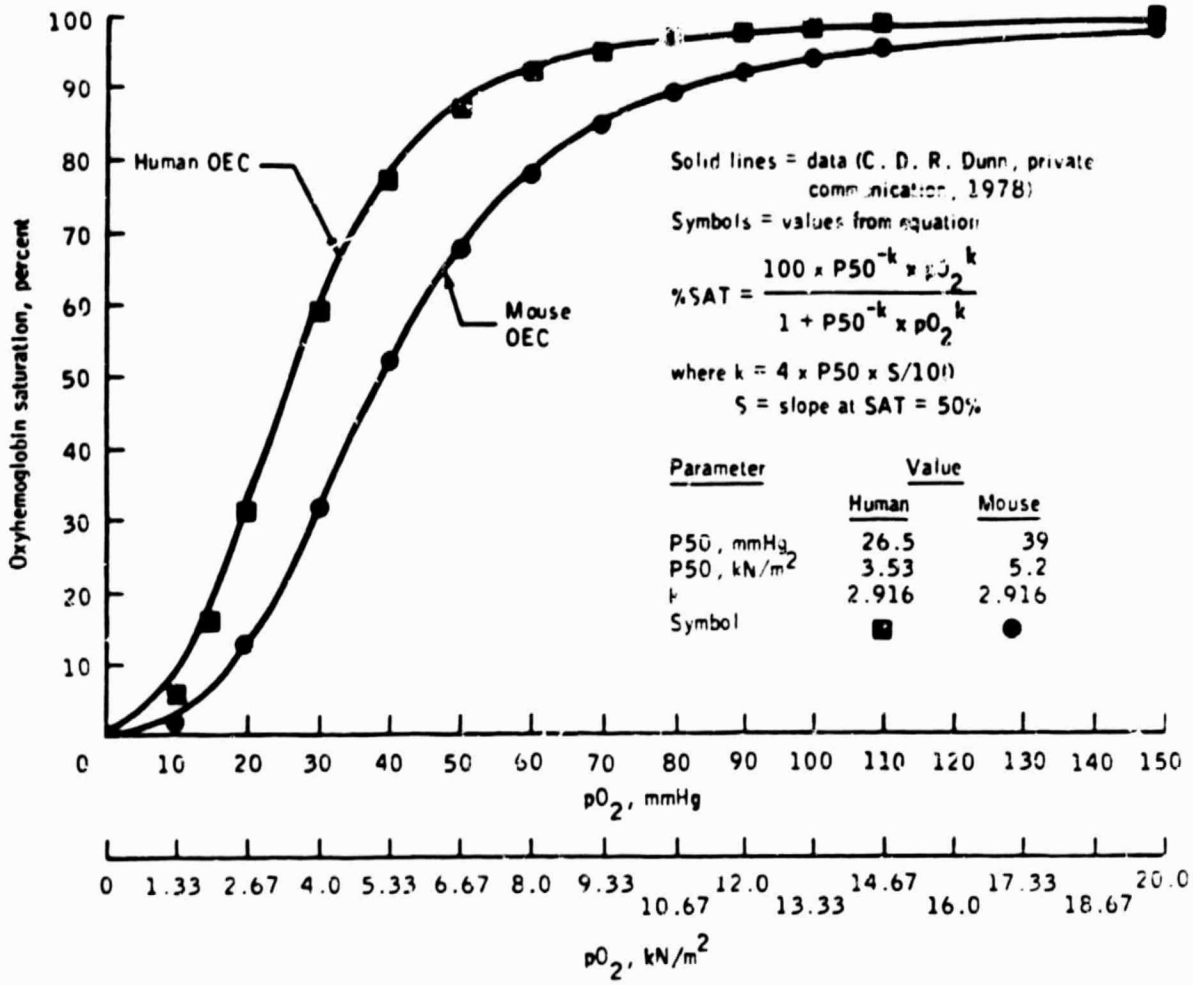

FIGURE B-8.—Oxygen-hemoglobin equilibrium curves for human and mouse: experimental versus theoretical values.

TABLE B-III.—Absolute Versus Specific Parameter Values

Parameter	Absolute units			Specific units[a]		
	Human	Mouse	Units	Human	Mouse	Units
Red cell mass	2000	0.63	ml	28.6	25.2	ml/kg body wt
Plasma volume	3000	.77	ml	42.9	30.8	ml/kg body wt
Blood volume	5000	1.40	ml	71.4	56.0	ml/kg body wt
Renal blood flow	1200	1.83	ml/min	4.28	6.10	ml min^{-1} g^{-1} tissue
Renal O_2 consumption	20	.04	ml/min	.073	133	ml min^{-1} g^{-1} tissue
Body O_2 consumption	250	.51	ml/min	.00357	0255	ml min^{-1} g^{-1} tissue

[a]Based on
Body weight = 70 kg man and 25 g mouse
Renal mass = 280 g (0.4 percent body wt) in man and 0.3 g (1.2 percent body wt) in mouse

Oxygen Balance

The balance of oxygen supply versus oxygen demand is crucial to the feedback regulation of erythropoiesis. A parameter reflecting this complex balance is the tissue oxygen tension that is believed to govern the release of erythropoietin. The oxygen balances for the human and mouse systems as used in the model are given in table B-IV.

Oxygen consumption per gram of renal tissue in the mouse is approximately twice that for the human. (Overall total oxygen consumption per gram body weight is nearly seven times greater in the mouse.) This higher oxygen demand of the mouse is satisfied in two ways in the model. First, there is a 50 percent greater efficiency in oxygen extraction as indicated in table B-IV. (Note that, in both species, the amount of oxygen delivered at rest is more than sufficient; i.e., roughly 10 times that required by the tissues.) Second, there is a 30 percent higher blood oxygen supply per gram of tissue because of greater tissue blood flow in the mouse.

TABLE B-IV.—Oxygen Balance at Kidney

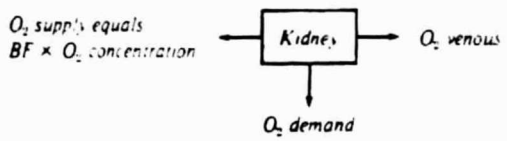

Parameter	Human	Mouse	Units
Oxygen demand	20	0.04	ml O_2/min
	073	153	ml O_2 min^{-1} g^{-1}
Oxygen supply			
pO_2, arterial	95	78	mmHg
	12 6*	10 4	kPa
sO_2, arterial	97 4	98 6	Percent saturation
O_2 concentration	196	188	ml O_2/liter blood
BF	1200	1 83	ml blood/min
O_2 supply rate	235	343	ml O_2/min
	839	1 143	ml O_2 min^{-1} g^{-1}
Oxygen venous			
pO_2, venous	56	57	mmHg
	7 4*	7 6	kPa
sO_2, venous	89	86	Percent saturation
pO_2, tissue	20	20	mmHg
	2 6*	2 6*	kPa
Percent oxygen extraction = (O_2 demand)/(O_2 supply)	8*	13 4	Percent

The normal tissue oxygen tension is arbitrarily assumed to be identical in both model systems, i.e., 2.67 kN/m² (20 mmHg). The equation describing oxygen diffusivity to the tissues from venous capillaries is given in the steady state as

$$\text{Net oxygen delivery} = \text{tissue oxygen consumption}$$

$$= \left(pO_2,\text{vein} - pO_2,\text{tissue}\right) \times K$$

where K = conductivity coefficient = O_2 diffusivity times the capillary surface area. The ratio K_{man}/K_{mouse} would be expected to reflect the surface area ratio between species if diffusivity is assumed similar in mouse and man. Therefore, if S is capillary surface area, then

$$\frac{S_{man}}{S_{mouse}} = \frac{K_{man}}{K_{mouse}}$$

$$= \frac{(O_2 \text{ consumption})_{man}}{(O_2 \text{ consumption})_{mouse}} \times \frac{(pO_2 \text{ vein} - pO_2 \text{ tissue})_{mouse}}{(pO_2 \text{ vein} - pO_2 \text{ tissue})_{man}}$$

$$= \frac{20 \text{ ml/min}}{0.04 \text{ ml/min}} \times \frac{(57.5 - 20) \text{ mmHg}}{(56.4 - 20) \text{ mmHg}}$$

$$= 515$$

This is in good agreement with the surface area ratio of 650 of the glomerulus derived from data in reference B-54 (p. 174), lending support to the general representation of the kidney in the computer model.

Functional Relationships

Three functional relationships are included in the computer model: (1) oxygen-hemoglobin equilibrium curve (OEC), (2) erythropoietin release as a function of tissue pO_2, and (3) erythrocyte production rate as a function of erythropoietin concentration. The first of these is shown in figure B-8 and will subsequently be described in detail. The form of the function curves for erythropoietin and red cell release will be assumed identical in the mouse and human models. There is no reason at the present time to take issue with this assumption, particularly since the bone marrow function was originally obtained from the mouse. These curves (as shown in figs.

B-2 and B-3 and as used in the models) are represented in normalized form (i.e., percent of control) so that any species may be represented. The gain factors G_1 and G_2, representing the slope of the relationships, may be different between species. This is of little concern in the basic design of the model because these parameters will be adjusted during the simulation process and their actual values will be estimated by "fitting" the model output to the experimental data.

The equation describing the sigmoidal OEC is a form of the Hill equation and is shown in the insert of figure B-8. The two solid lines represent human and mouse blood, respectively, and were recently obtained from blood samples of the C3H mouse (ref. B-49). The value of $P50$ is explicitly stated in the equation so that shifts in oxygen-hemoglobin affinity may be easily described. The value of the exponent k, found from the best fit of the mouse curve, also provides a good fit of the human curve as shown in figure B-8. Thus, the only difference between the equation describing the human and mouse OEC is the value of $P50$.

REFERENCES

B-1 Adamson, J. W., and Finch, C. A. Hemoglobin Function, Oxygen Affinity, and Erythropoietin. Ann. Rev. Physiol., vol. 37, 1975, pp. 351-369.

B-2 Fisher, J. W., Buisuttil, R., et al. The Kidney and Erythropoietin Production: A Review. Erythropoiesis—Proceedings of the Fourth International Conference on Erythropoiesis, K. Nakao, J. W. Fisher, and F. Takaku, eds., University Park Press, 1975, pp. 315-336.

B-3 Jacobson, L. O., Goldwasser, E., Fried, W., and Plzak, L.: Role of the Kidney in Erythropoiesis. Nature, vol. 179, 1957, pp. 633-634.

B-4 Finch, Clement A., and Lenfant, Claude: Oxygen Transport in Man. New England J. Med., vol. 286, no. 8, 1972, pp. 407-415.

B-5 Hodgson, G.: Application of Control Theory to the Study of Erythropoiesis. Regulation of Hematopoiesis, Vol. 1, ch. 15, A. S. Gordon, ed., Appleton-Century-Crofts (New York), 1970.

B-6 Beutler, E.: "A Shift to the Left" or "A Shift to the Right" in the Regulation of Erythropoiesis. Blood, vol. 33, 1969, pp. 496-500.

B-7 Krantz, S. B., and Jacobson, L. O.: Erythropoietin and the Regulation of Erythropoiesis. University of Chicago Press, 1970.

B-8 Reissman, K. R., Diederich, Dennis A., Ito, Kenjiro, and Schmaus, John W.: Influence of Disappearance Rate and Distribution Space on Plasma Concentration of Erythropoietin in Normal Rats. J. Lab. & Clin. Med., vol. 65, 1965, pp. 967-975.

B-9 Van Dyke, D. C., and Pollycove, M.: The Relation of Erythropoietin to Anemia and Polycythemia. Erythropoiesis, L. O. Jacobson and M. Doyle, eds., Grune and Stratton (New York), 1962, pp. 340-350.

B-10 Harris, J. W., and Kellermeyer, R. W.: The Red Cell: Production, Metabolism, Destruction, Normal & Abnormal. Harvard University Press (Cambridge), 1970.

B-11 Finch, C. A., Denbelbeiss, K., et al.: Ferrokinetics in Man. Medicine, vol. 49, 1970, pp. 17-53.

B-12 Peschle, C., Marone, G., Sacchetti, L., and Condorelli, M.: The Hormonal Influences on Red Cell Production: Physiological Significance and Mechanism of Action. Erythropoiesis—Proceedings of the Fourth International Conference on Erythropoiesis, K. Nakao, J. W. Fisher, and F. Takaku, eds., University Park Press, 1975, pp. 99-117.

B-13 Baciu, I.: The Humoral and Neural Regulation of Erythropoiesis. Translation of "Die humorale und nervose Regelung der Erythropoese." Klinische Wochenschrift, vol. 48, no. 3, 1970, pp. 133-143 (NASA TT F-13, 157).

B-14 Gordon, A. S., and Zanjani, E. D.: Some Aspects of Erythropoietin Physiology. Regulation of Hematopoiesis, Vol. 1, ch. 19, A. S. Gordon, ed., Appleton-Century-Crofts (New York), 1970.

B-15 Guyton, A. C., Coleman, T. G., and Granger, H. J.: Circulation: Overall Regulation. Ann. Rev. Physiol., vol. 34, 1972, pp. 13-46.

B-16 Middleman, S.: Transport Phenomena in the Cardiovascular System. Wiley-Interscience (New York), 1972, pp. 1-115.

B-17 Mylrea, Kenneth C., and Abbrecht, Peter H.: Mathematical Analysis and Digital Simulation of the Control of Erythropoiesis. J. Theor. Biol., vol. 33, no. 2, Nov. 1971, pp. 279-297.

B-18 Adamson, J. W.: The Erythropoietin Hematocrit Relationship in Normal and Polycythemic Man: Implications of Marrow Regulation. Blood, vol. 32, no. 4, 1968, pp. 597-609.

B-19 Ersley, A. J.: Erythropoietin in Clinical Medicine. Erythropoiesis—Proceedings of the Fourth International Conference on Erythropoiesis, K. Nakao, J. W. Fisher, and F. Takaku, eds., University Park Press, 1975, pp. 425-433.

B-20 Waldman, Th Discussion on the Metabolic Fate of Erythropoietin Erythropoiesis. L O Jacobson and M Doyle, eds Grune and Stratton (New York), 1962, pp 136-137

B-21 Riggs, D S Control Theory and Physiological Feedback Mechanisms Williams and Wilkins Co (Baltimore), 1970

B-22 Camiscoli, J F., and Gordon, A S Bioassay and Standardization of Erythropoietin Regulation of Hematopoiesis, Vol 1, A S Gordon, ed., Appleton-Century-Crofts (New York), 1970, pp 369-394.

B-23 Gurney, C W., Degowin, R., Hofstra, D., and Byron, J Application of Erythropoietin to Biological Investigation Erythropoiesis, L O Jacobson and M Doyle, eds., Grune and Stratton (New York), 1962, pp 151-161

B-24 Dunn, C D R., Jones, J B, Jolly, J D., and Lange, R D Progenitor Cells in Canine Cyclic Hematopoiesis Blood, vol 50, 1977, pp 1111-1120

B-25 Berlin, N I Life Span of the Red Blood Cell The Red Blood Cell, ch 12, C Bishop and D M Surgenor, eds, Academic Press (New York), 1964

B-26 Mackey, M C Unified Hypothesis for the Origin of Aplastic Anemia and Periodic Hematopoiesis Blood, vol 51, 1978, pp 941-956

B-27 King-Smith, E A, and Morley, A Computer Simulation of Granulopoiesis Normal and Impaired Granulopoiesis Blood, vol 36, 1970, pp 254-262

B-28 Arden, B W, and Astill, K N Numerical Algorithms Origins and Applications Addison-Wesley Publishing Co (Reading, Mass), 1970

B-29 Aberman, A, Cavanilles, J M., et al An Equation for the Oxygen Hemoglobin Dissociation Curve J Appl Physiol, vol 35, no 4, 1973, pp 570-571

B-30 Leonard, J I Dynamic Regulation of Erythropoiesis A Computer Model of General Applicability Rep TIR 741-LSP-9005, General Electric Co (Houston, Tex.), 1979

B-31 Kimzey, S L, Leonard, J I, and Johnson, P C A Mathematical and Experimental Simulation of the Hematological Response to Weightlessness Acta Astronaut, vol 6, 1979, pp 1289-1303

B-32 Guyton, A C, Coleman, T G, et al Relationship of Fluid and Electrolytes to Arterial Pressure Control and Hypertension Quantitative Analysis of an Infinite-Gain Feedback System Hypertension Mechanisms and Management, G Onesti, K E Kim, and J H Moyer, eds, Grune and Stratton (New York), 1973

B-33 Grant, Wilson C, and Root, Walter S Fundamental Stimulus for Erythropoiesis Physiol Rev, vol 32, 1952, pp 449-498

B-34 Adamson, John W., Parer, Julian T, and Stamatoyannopoulous, George Erythrocytosis Associated With Hemoglobin Rainier Oxygen Equilibria and Marrow Regulation J Clin Invest, vol 48, no 3, 1969, pp 1376-1386

B-35 Metcalfe, James, and Dhindsa, Dharam S The Physiological Effects of Displacements of the Oxygen Dissociation Curve Oxygen Affinity of Hemoglobin and Red Cell Acid Base Status, P Astrup and M Rorth, eds, Academic Press (New York), 1972, pp 613-628

B-36 Aperia, A C., Liebow, A A., and Roberts, L E. Renal Adaptation to Anemia Circulation Res., vol 22, 1968, pp 489-500

B-37 Selkurt, E E The Renal Circulation Handbook of Physiology, Sec 2 Circulation, vol 2, W F Hamilton and Philip Dow, eds, ch 43, American Physiological Society (Washington, D C), 1963.

B-38 Pitts, R F Physiology of the Kidney and Body Fluids Second ed Yearbook Medical Publishers (Chicago), 1968

B-39 Granger, Harris J, Goodman, Anthony H., and Cook, Billy H Metabolic Models of Microcirculatory Regulation Fed Proc, vol 34, no 11, 1975, pp 2025-2030

B-40 Duvelleroy, M A, Mehmel, H., and Laver, M B Hemoglobin-Oxygen Equilibrium and Coronary Blood Flow An Analog Model J Appl Physiol, vol 35, no 4, 1973, pp 480-484

B-41 Thorling, E B, and Ersley, A J The "Tissue" Tension of Oxygen and Its Relation to Hematocrit and Erythropoiesis Blood, vol 31, 1968, pp 332-343.

B-42 Parer, J T Oxygen Transport in Human Subjects With Hemoglobin Variants Having Altered Oxygen Affinity Respir Physiol, vol 9, 1970, pp 43-49.

B-43 Dunn, C D R, and Lange, R D Erythropoietic Effects of Space Flight Acta Astronaut., vol 6, May-June 1979, pp 725-732

B-44 Kretchmar, A L Erythropoietin Hypothesis of Action Tested by Analog Computer Science, vol 152, 1966, pp 367-370

B-45 Ersley, A J, and Silver, R K Compensated Hemolytic Anemia Blood Cell, vol 1, 1975, pp 509-525.

B-46 Lajtha, L G, Oliver, R., and Gurney, C W Kinetic Model of a Bone-Marrow Stem-Cell Population British J Hematol, vol 8, 1962, pp 442-460

B-47 Leonard, J I Study Report—Improvements and Validation of the Erythropoiesis Control Model for the Simulation of Bed Rest (General Electric Co, Houston, Tex.; TIR 741-LSP-7012) NASA CR-160187, 1977

B-48. Leonard, J. I.: System Parameters for Erythropoiesis Control Model: Comparison of Normal Values in Human and Mouse Model. (General Electric Co., Houston, Tex.: TIR 741-LSP-8024.) NASA CR-160401, 1978.

B-49. Dunn, C. D. R.: Effect of Dehydration on Erythropoiesis in Mice: Relevance to the "Anemia" of Space Flight. Aviat. Space & Environ. Med., vol. 49, 1978, pp. 990-993.

B-50. Green, Earl L., ed.: Biology of the Laboratory Mouse. McGraw-Hill (New York), 1967, pp. 351-372.

B-51. Altman, Philip L.; and Dittmer, Dorothy S.: Biology Data Handbook, vols. 1, 2, and 3. Federation of American Societies for Experimental Biology (Bethesda, Md.), 1972.

B-52. Ulrich, S.; Hilpert, P.; and Bartels, H.: Uber die Atmungrfunktion des Blutes von Spitzmausen wuBen Mausen und syrischen Goldhamstern. Pflugers Arch., vol. 277, 1963, pp. 150-165.

B-53. Abbrecht, Peter H., and Littell, Judith K.: Erythrocyte Life Span in Mice Acclimatized to Different Degrees of Hypoxia. J. Appl. Physiol., vol. 32, no. 4, 1972, pp. 443-445.

B-54. Spector, William S.: Handbook of Biological Data. W. B. Saunders Co. (Philadelphia), 1961, p. 174.

B-55. Arendshorst, William F.: Autoregulation of Blood Flow in the Rat Kidney. American J. Physiol., vol. 228, no. 1, 1975, pp. 127-133.

B-56. Abbrecht, Peter H.; and Littell, Judith K.: Plasma Erythropoietin in Men and Mice During Acclimatization to Different Altitudes. J. Appl. Physiol., vol. 32, no. 1, 1972, pp. 54-58.

Also see:

Leonard, J.I.; Kimzey, S.L. and Dunn, C.D.R. Dynamic Regulation of Erythropoiesis: A Computer Model of General Applicability. Expt. Hematol. Vol. 9, 1981, pp. 355-378. (Primary source - Leonard, J.I. TIR 741-LSP-9005, General Electric Co., NASA CR-160203, 1979)